Research Square

Preprints are preliminary reports that have not undergone peer review.
They should not be considered conclusive, used to inform clinical practice,
or referenced by the media as validated information.

A blend of lemongrass, clove, and thyme essential oils encapsulated in hydroxypropyl methylcellulose nanofibers by electrospinning: characterization and biological activity

Lisiane Pintanela Vergara
lisianevergara@yahoo.com.br
Universidade Federal de Pelotas
Kátia Gomes da Silva
Universidade Federal de Pelotas
Cristina Jansen-Alves
Universidade Federal de Pelotas
Elder Pacheco da Cruz
Universidade Federal de Pelotas
Tatiane Jéssica Siebeneichler
Universidade Federal de Pelotas
Glória Caroline Paz Gonçalves
Universidade Federal de Pelotas
Tamires Soares Schug
Universidade Federal de Pelotas
Laura de Vasconcelos Costa
Universidade Federal de Pelotas
Flavia Tayna Serra Silva
Universidade Federal de Pelotas
Gabriela Niemeyer Reissig
Brazilian Agricultural Research Corporation
Elessandra da Rosa Zavareze
Universidade Federal de Pelotas
Deborah Murowaniecki Otero
Universidade Federal da Bahia
Eliezer Ávila Gandra
Universidade Federal de Pelotas
Leonardo Nora
Universidade Federal de Pelotas
Rui Carlos Zambiazi

Research Article

Keywords: DPPH, Escherichia coli, Staphylococcus aureus, Aspergillus flavus, Botrytis cinerea, Penicillium crustosum

Posted Date: July 27th, 2026

DOI: https://doi.org/10.21203/rs.3.rs-10425332/v1

License: This work is licensed under a Creative Commons Attribution 4.0 International License. Read Full License

Additional Declarations: No competing interests reported.

Abstract

The objective of this study was to encapsulate a blend of essential oils (EOs), comprising lemongrass, clove, and thyme, in hydroxypropyl methylcellulose (HPMC)-based nanofibers using the electrospinning technique. Nanofibers were produced incorporating different concentrations of EOB (0, 5, 10, 15, and 20% w/w) relative to HPMC. The nanofibers were evaluated for morphology and size distribution (SEM), load capacity (LC), encapsulation efficiency (EE), contact angle, DSC, FTIR, antioxidant activity, antibacterial activity, and antifungal activity. The nanofibers exhibited a cylindrical, homogeneous morphology without bead-like defects; however, at the highest EOB concentrations (15 and 20%), they showed a tendency toward structural collapse/flattening with average diameters ranging from 62.96 to 160.35 nm. The nanofibers exhibited low contact angles with water, ranging from 11.21 to 58.96˚. The FTIR spectra of the nanofibers showed bands characteristic of their constituents (HPMC and EOB). The highest LC value was obtained for the nanofiber containing 5% EOB (58.5%), accompanied by a high EE (94.2%). The blend proved to be more thermally stable when incorporated into the nanofibers than in its non-encapsulated form. Pure EOB and the nanofiber containing 20% EOB exhibited high antioxidant activity using the DPPH radical method. The nanofibers with 10% and 15% EOB showed the greatest inhibitory effect against *S. aureus* and *E. coli*. The nanofibers containing 15% and 20% EOB exhibited 100% inhibition against the fungus *Botrytis*. Therefore, HPMC-EOB nanofibers are promising antibacterial and antifungal agents in the food industry, with potential for both replacing synthetic additives and for packaging production.

1 Introduction

With the growing demand for natural products, plant extracts such as essential oils (EOs) have gained prominence for their effectiveness as antimicrobial and antifungal agents. Many of these oils have been recognized as “Generally Recognized as Safe” (GRAS) by the U.S. Food and Drug Administration (FDA) (Magri et al., 2025). Due to their chemical composition, essential oils are susceptible to degradation under the influence of various factors, such as light, temperature, pH, humidity, oxygen, and volatilization, which limit their direct application (Fonseca et al., 2020). In this regard, encapsulation offers an alternative technology that provides protection and increased stability for active compounds, traps essential oils within a protective matrix, thereby improving their stability, bioavailability, and controlled release (Laina et al., 2024).

The encapsulation of essential oils can be performed individually or in blends, combining their functional properties to enhance the desired effect. The use of essential oil blend (EOB) is a promising approach, as it can broaden their chemical composition and create multiple mechanisms of action, leading to highly desirable synergistic effects for food preservation through multiple biochemical processes, as well as antibacterial and antifungal activity (Shamene et al., 2024).

Various techniques are used to encapsulate essential oils, notably the electrospinning technique, which serves as an alternative to increase the stability of these highly temperature-sensitive compounds, since the process is conducted at room temperature, thereby preserving the biological, antimicrobial, and antioxidant activity of the encapsulated compounds in structures in the form of nanofibers or nanocapsules (Wen et al., 2017). The technique is considered simple and low-cost and can be developed using natural polymers, biodegradable and biocompatible, as well as synthetic polymers, proteins, polysaccharides, and others

(Estevam, 2022). However, biodegradable polymers are preferred in electrospinning due to their environmentally friendly nature. Among the various polymers, hydroxypropyl methylcellulose (HPMC), a cellulose derivative, is hydrophilic and can be used in various food industry applications as a thickening agent, emulsifier, stabilizer, and primarily for providing controlled release of encapsulated compounds (Ding et al., 2015). Few studies report the production of hydroxypropyl methylcellulose (HPMC) nanofibers for encapsulating a blend of essential oils, and none were found combining lemongrass, clove, and thyme essential oils in HPMC nanofibers via electrospinning.

Lemongrass essential oil (LEO) (*Cymbopogon flexuosus*) is well known for its strong lemon aroma due to its high citral content, around 75%, and for its antioxidant and antimicrobial potential against fungi, yeasts, and bacteria (Kieling & Prudencio, 2019). Magri et al. (2025) identified specific compounds in LEO, the major ones being α-citral, followed by citronellal and citronellol. Research by Jafari et al. (2025) revealed that LEO exhibited antimicrobial effects against *E. coli*, *Staphylococcus aureus*, *Lactobacillus curvatus*, *S.* typhimurium, and *Aspergillus niger*. Clove essential oil (CEO) (*Syzygium aromaticum*) contains eugenol, which is responsible for its analgesic, anti-inflammatory, and antioxidant activity, and also has a high content of bioactive compounds (da Silva Scudeler et al., 2020). Thyme essential oil (TEO) (*Thymus vulgaris* L.) contains a high content of polyphenols and includes thymol and carvacrol in its composition, which are phenolic compounds responsible for antimicrobial effects (Guarda et al., 2011). Navikaite-Snipaitiene et al. (2025) analyzed clove and thyme essential oils and observed inhibitory effects against *E. coli* followed by *L. monocytogenes*. This comprehensive understanding of the bioactive composition and the antimicrobial and antifungal properties of lemongrass, clove, and thyme essential oils reinforces their potential for application in various fields (dos Santos et al., 2024). Several studies have demonstrated the use of these essential oils to preserve and extend the shelf life of food products, thereby encouraging the replacement of chemical additives (da Cruz et al., 2023; Souza et al., 2025).

In this regard, the combination of lemongrass, clove, and thyme essential oils may promote synergistic effects, enhancing antimicrobial activity through the combined action of their components (Al-Refaie et al., 2023; Bouqellah et al., 2025). Bouqellah et al. (2025) demonstrated that the encapsulation of essential oils from *Allium sativum* and *Cinnamomum verum* in silver nanoparticles (AgNPs) significantly increased their antifungal efficacy against *Botrytis cinerea*.

Thus, the objective of this study was to characterize the antimicrobial and antifungal activity of lemongrass, clove, and thyme essential oils, and to incorporate a blend of these oils into hydroxypropyl methylcellulose (HPMC) nanofibers via electrospinning, with a view to potential applications as an active system in food products and active packaging.

2 Materials and Methods

2.1 Materials

Three commercial essential oils from different botanical sources were used: lemongrass (*Cymbopogon flexuosus*, CAS: 91844-92-7), clove (*Eugenia caryophyllus*, CAS: 8015-97-2), and thyme (*Thymus vulgaris*, CAS: 8007-46-3). The essential oils were purchased from Ferquima®, all extracted by hydrodistillation according to

the products' technical specifications. The polymer used for nanofibers production was hydroxypropyl methylcellulose (E10M HPMC Type, 822013, methoxyl 28–30%, hydroxypropyl 7–12%, 2% wet-strength solution, 20°C, 7,500–14,000 mPa·s, kDa) of the Ashland® AquaSolveTM brand. Absolute ethyl alcohol purchased from Dinâmica® Química Contemporânea LTDA (99.5% purity, CAS: 64-17-5) and distilled water were the solvents used to dissolve the HPMC solutions. The other reagents used were of analytical grade.

2.2 In vitro antimicrobial activity of essential oils (EOs)

The antimicrobial activity of lemongrass, clove, and thyme essential oils was evaluated using three phenotypic methods: disk diffusion, minimum inhibitory concentration (MIC), and minimum bactericidal concentration (MBC). The antimicrobial effects of lemongrass, clove, and thyme essential oils (EOs) were tested on standard strains of the bacterial species *Escherichia coli* (*E. coli*) (ATCC 25922 and INQS 00182) and *Staphylococcus aureus* (*S. aureus*) (ATCC 10832).

2.2.1 Agar diffusion disk test for essential oils (EOs)

The disk diffusion assay was performed according to the protocol proposed by the Clinical and Laboratory Standards Institute Manual (CLSI, 2012), with minor modifications. To prepare the cultures, a loopful of each bacterial strain was transferred to a tube containing trypticase soy broth (TSB, Kasvi, Italy) and incubated for 24 hours at 37°C. Afterwards, a loopful of this growth was streaked onto Petri dishes containing selective media, methylene blue eosin agar (EMB) for *E. coli* and Baird-Parker agar for *S. aureus*, and incubated for 24 h at 37°C to isolate the colonies. From the bacterial growth in TSB broth, 1 mL was withdrawn, resuspended in 10 mL of saline solution (0.85% NaCl, Synth, Brazil), and standardized to a turbidity standard of 0.5 on the McFarland scale (1.5×10^8 CFU/mL). For the diffusion disk assay, the inoculum-containing saline solution was streaked onto the surface of Müller-Hinton (MH) agar plates (Kasvi, Brazil) using a sterile swab. Next, sterilized filter paper discs (Laborclin, Brazil) with a diameter of 6 mm were added. After 10 µL of the essential oils were placed on the filter paper discs (Laborclin, Brazil), all plates were sealed with parafilm and incubated for 24 h at 37°C. Immediately after the incubation period, the inhibition zones were measured with a universal caliper (FORTG, FG8330, Brazil), and the results were expressed in millimeters (mm). All assays were performed in triplicate.

2.2.2 Minimum inhibitory concentration (MIC) and minimum bactericidal concentration (MBC)

The minimum inhibitory concentration (MIC) and minimum bactericidal concentration (MBC) were determined according to the protocol proposed by the Clinical and Laboratory Standards Institute Manual (CLSI, 2012), with minor modifications. For this purpose, 96-well microtiter plates were used, to which 260 µL of Brain Heart Infusion broth (BHI, HiMedia, India), 20 µL of saline solution standardized with an inoculum of each bacterium, 20 µL of Tween 80, and 20 µL of EO were added to the wells, and dilutions of the oil were performed across the wells on the plate. After sample preparation, the microtiter plates were read on a spectrophotometer (Molecular Devices, SpectraMax 190, USA) at 625 nm. The plates were then incubated for 24 h at 37°C. After incubation, the plates were re-evaluated by spectrophotometry under the same conditions. The MIC of the essential oil was defined as the lowest concentration at which no bacterial growth was observed in the BHI broth (optical density of the sample less than or equal to the initial reading, obtained by comparing, in each

well, the initial readings with those after incubating the plate in the incubator), with results expressed in mg/mL. To determine the minimum bactericidal concentration (MBC), 15 µL aliquots were taken from wells showing inhibition of bacterial growth for *E. coli* or *S. aureus*, streaked onto Petri dishes containing Müller-Hinton (MH) agar (Kasvi, Brazil), and incubated at 37°C for 24 h. The minimum bactericidal concentration was defined as the concentration at which no bacterial growth was observed on Mueller-Hinton agar, and results were expressed in mg/mL.

2.3 *In vitro* antifungal activity of essential oils (EOs)

The antifungal effect was evaluated using a contact assay. The antifungal effects of the oils were tested on cultures of the fungi *Aspergillus flavus*, *Botrytis cinerea*, and *Penicillium crustosum*.

2.3.1 Antifungal activity of essential oils (EOs) via contact action

The antifungal activity was evaluated using the methodology described by Tao et al. (2014) and Chen et al. (2025), with some modifications. First, cultures of the fungi *Aspergillus flavus*, *Botrytis cinerea*, and *Penicillium crustosum*, previously stored on potato dextrose agar (PDA) under refrigeration (at 5°C), were transferred to a Petri dish containing the same culture medium and incubated at 25°C for 5 days in a germination chamber (SolidSteel, SSGFa, Brazil). After the five-day incubation period, a loopful of the fungal cultures from the Petri dishes was extracted and resuspended in 2 mL of sterile saline solution (0.8% NaCl w/v, Synth, Brazil), which was standardized to 0.5 on the McFarland scale (1.5×10^8 CFU mL^{-1}). The essential oils were added directly to the medium before it was poured into sterilized Petri dishes (90 x 15 mm) for direct contact action. For the contact action method, concentrations ranging from 1 to 0.6 µL/mL of the tested essential oils were used. A solution of sterile distilled water and Tween 80 (1%, v/v) was prepared and added to the culture medium to ensure equal volume and uniform distribution of the added oil across all treatments. Plates with growth (without EO) were used as positive controls, and plates without growth were used as negative controls. All Petri dishes were inoculated with cultures of the fungi *Aspergillus flavus*, *Botrytis cinerea*, and *Penicillium crustosum*, obtained from the edge of a fungal colony, using a cork borer (a 5-mm “fungal disc” removed from the plate). The plates were sealed with parafilm and incubated upside down at 25°C. All treatments were performed in triplicate. After 72 h of incubation, the colony diameter was measured as the distance between the diametrically opposite edges of the fungal colony on the plates using a universal caliper (FORTG, FG8330, Brazil) (cm). The percentage of mycelial growth inhibition (PGI) was calculated according to Eq. 1.

Eq. 1

$$\text{IMG (\%)} = \frac{dc - dt}{dc - 0.5} \times 100$$

where dc (cm) is the average colony diameter for controls and dt (cm) is the average colony diameter for the treatment. The results are expressed as the mean ± standard deviation.

2.4 Preparation and evaluation of the volatile compound profile of the essential oil blend

The essential oil blend (EOB) was prepared based on the results of the individual essential oils, with the selection criterion being the best balance of antimicrobial and antifungal activity. The EOB was prepared in a 50:25:25 ratio (v/v/v), corresponding respectively to 250 µL of lemongrass oil, 125 µL of clove oil, and 125 µL of thyme oil, which were mixed and homogenized in a vortex mixer (Phoenix, AP-56, Brazil) for 1 min, then stored in an amber bottle and kept refrigerated at 4°C until the time of analysis.

The chemical composition of the EOB was analyzed by gas chromatography coupled with mass spectrometry (GC-MS), using a Shimadzu QP2010 Ultra GCMS system with an AOC-20i autosampler (Japan). The injection, chromatographic separation, and detection parameters were adjusted according to Juliani et al. (2008). The EOB were injected in split mode (1:50), with an injector temperature of 200°C. Helium gas, used as the carrier gas, was maintained at a flow rate of 1.08 mL/min and controlled by linear velocity. An Rtx-1MS capillary column (30 m × 0.32 mm × 0.25 µm) was used, initially operated under isothermal conditions at 60°C for 1 minute, followed by a heating ramp of 5°C/min up to 180°C, with the temperature maintained for an additional 1 min. The total run time was 26 minutes. The ion source and interface were maintained at 200°C with a scan rate of 0.2 scans/s. The analyzed compounds were in the range of 40 to 450 m/z, and for each compound, the retention time, similarity index, and mass spectrum were analyzed and compared with the GC/MS system database (NIST11s.lib). Compound identification was based on the percentage ratio of peak area to peak height and on the mass spectra.

2.5 Preparation of polymer solutions

The polymer solutions used to incorporate the blend of essential oils (lemongrass, clove, and thyme) were prepared using the biopolymer hydroxypropyl methylcellulose (HPMC) as the wall material. HPMC solutions were prepared at a concentration of 3% (w/v) by weighing 0.24 g of HPMC into 8 mL of 70% ethanol (v/v in distilled water), followed by stirring for 48 h using a magnetic stirrer (Velp Scientifica, Multistirrer 6, Italy) to ensure complete solubilization of the HPMC.

Varying amounts of EOB were incorporated into the HPMC polymer solution and agitated for 30 min under agitation, protected from light, prior to electrospinning. The EOB were prepared in a 50:25:25 (v/v/v) ratio, corresponding to lemongrass, clove, and thyme oils, respectively. The amounts of EOB incorporated were calculated based on the initial mass of HPMC used (0, 5, 10, 15, and 20% w/w), corresponding to approximately 0.2, 0.4, 0.6, and 0.8 g of EOBs in 4 g of the final polymer solution.

2.6 Yield from nanofiber production

The fiber production yield was determined according to the method proposed by Pires et al. (2024), with some adaptations. Initially, the polymer solution was prepared using approximately 0.24 g of HPMC in 8 mL of 70% (v/v) ethanol and stirred for 48 h. The empty flask and, subsequently, the flask containing HPMC and 70% ethanol were weighed, and the difference between these masses was used to determine the mass of the initial polymer solution.

For the preparation of formulations containing 0, 5, 10, 15, and 20% EOB, 4 g of the initial polymer solution were weighed, and approximately 0.2, 0.4, 0.6, and 0.8 g of EOB were added, respectively. The dispersions were stirred for 30 min, protected from light, prior to electrospinning. The plastic syringe containing each

polymer solution, together with the needle, and the aluminum foil used as the collector were weighed before electrospinning and after 1 h of fiber collection.

For the control nanofiber (0% EOB), the yield (%) was calculated considering the fraction of HPMC present in the initial polymer solution, the mass of solution effectively injected during electrospinning (obtained from the difference in mass of the syringe and needle before and after the process), and the mass of nanofibers collected (determined from the difference in mass of the aluminum foil before and after collection).

For the formulations containing 5, 10, 15, and 20% EOB, the calculation initially considered the fraction of HPMC present in the initial polymer solution and its corresponding mass in the 4 g of solution used. Subsequently, the fractions of HPMC and EOB in the final polymer solution were determined. Based on the mass of solution effectively injected, the masses of HPMC and EOB introduced into the system were calculated. Finally, the yield (%) was obtained by relating the mass of nanofibers collected after 1 h of electrospinning to the total mass of solids injected into the system (HPMC + EOB), multiplied by 100.

2.7 Electrical Conductivity and Rheology of HPMC-EOB Polymer Solutions

Polymer solutions prepared with different concentrations (0%, 5%, 10%, 15%, and 20%) of EOB were evaluated for their rheology and electrical conductivity. The electrical conductivity (κ) of the polymer solutions was measured using a conductivity meter (Simpla EC150, China), and the results were reported in μS cm^{-1}.

For the rheological test, under steady-state conditions, approximately 0.7 mL of the polymer solution was dispensed onto a stationary, horizontal flat plate attached to a rotational rheometer (Brookfield Engineering Laboratories, MA 02346, USA). The measurement geometry ($C50^{-1}$ sensor) used in the test was of the cone-and-plate type (50 mm radius), with a gap of 0.05 mm and α ≈ 1°. For the sweep, a shear rate ramp from 0 to 60 s^{-1} was used, with test times ranging from 0.1 to 300 s, at 25°C and local atmospheric pressure. The data obtained were analyzed using Rheo 3000 v1.2 software. The rheological parameters were modeled using the Power Law model, as described in Eq. 2. The performance of the Power Law model in fitting the rheological data was evaluated using accuracy metrics, namely the coefficient of determination (R^2) and the mean percentage deviation (P). The characterization of the polymer solution was performed at room temperature (25 ± 2°C).

Eq. 2

$$\tau = K\dot{\gamma}^{n}$$

where τ is the shear stress (Pa), K is the consistency index or apparent viscosity of the fluid (Pa·s^n), $\dot{\gamma}$ is the strain rate or shear rate (s^{-1}) and n is the flow behavior index (dimensionless).

2.8 Encapsulation of HPMC-EOB nanofibers by electrospinning

The polymer solutions were loaded into a 3-mL plastic syringe fitted with a stainless-steel spinneret needle (Ø 0.8 mm) that was pointed horizontally toward a grounded stainless steel collection plate. The nanofibers were produced on a laboratory-scale horizontal electrospinning station, which included an infusion pump (KD

Scientific, Model 100, England), a high-voltage DC power supply (Faíscas, FA+30kV, Brazil), and a metal collector covered with aluminum foil. The process parameters used during nanofibers production were a voltage of 28 kV, a 15 cm distance between the needle and a collector, and a polymer solution pumped at a constant flow rate of 1 mL/h. The conditions used were room temperature set to 18 ± 1°C using an air conditioner (Electrolux, EcoTurbo, Brazil), and relative humidity was set to 40 ± 5% RH using an air dehumidifier (Quimis, Q831M 20, Brazil). The parameters chosen were based on the methodology proposed by da Silva et al. (2025).

2.9 Morphology and Size Distribution of HPMC-EOB nanofibers

The morphology was determined using a scanning electron microscope (SEM) (JEOL, JSM-6610LV, United States). The samples were mounted on stubs, metalized with gold using a sputtering system (Denton Vacuum Desk V, USA) at 20 mA for 120 s, and analyzed at an acceleration voltage of 10 kV. Microscopic images were captured at magnifications of 500, 1000, 5000, 10,000, and 20,000x. The nanofibers size distribution and average diameter were determined using ImageJ (version 221, 1.8.0_172) by measuring 60 randomly selected nanofibers from the micrographs da Silva et al. (2025).

2.10 Contact angle of HPMC-EOB nanofibers

The contact angle was measured to investigate the adhesion of liquids to the materials using the sessile drop technique, and the static contact angle (θ) was measured using a goniometer (Labometric, LB-DX, United States) at room temperature (22 ± 2°C) and 73% RH. The hydrophilicity/hydrophobicity of HPMC membranes incorporated with EOB (0, 5, 10, 15, and 20%) was determined using the electrospinning technique. The membranes were deposited onto glass slides for further analysis. A 7 µL drop of ultrapure water, obtained using a water purification system (Milli-Q®, Synergy®, Canada), was placed on the sample, and the drop's absorption time was recorded from time zero, the moment the drop fell, until 30 seconds of contact between the drop and the nanofibers membrane. The material was photographed with the digital camera, which is part of the equipment, at 20 FPS (frames per second) in a consistent lighting condition and camera distance for each sample. θ was calculated using the OneAttension software da Silva et al. (2025).

2.11 Fourier-transform infrared (FT-IR) spectra of HPMC-EOB nanofibers

The functional groups present in the EOB and in the HPMC nanofibers incorporating different concentrations of EOB (0, 5, 10, 15, and 20%) were analyzed by Fourier-transform infrared spectroscopy (FTIR) in attenuated total reflectance (ATR) mode, using a Shimadzu IRPrestige-21 spectrometer. The samples were analyzed directly on the ATR diamond crystal, applying uniform pressure to ensure adequate contact with the surface. The spectra were obtained over 4000 – 650 cm^{-1}, with a resolution of 4 cm^{-1} and an average of 32 scans per spectrum. The ATR crystal was cleaned with isopropyl alcohol between samples to prevent contamination.

2.12 Load capacity (LC) and encapsulation efficiency (EE) of HPMC-EOB nanofibers

The content of surface EOB compounds was determined according to the method described by Vitoria et al. (2025). External EOB compounds were quantified by washing 50 mg of nanofibers with 5 mL of hexane under gentle agitation for 10 seconds. The mixture was centrifuged at 3226 × g for 5 min, and the supernatant was collected. The compounds were analyzed using a Shimadzu GC/MS QP-2010 (Shimadzu Corporation, Kyoto, Japan) equipped with an AOC-20i autosampler and the NIST mass spectrum library, 2011. To determine the total content of EOB compounds (due to fiber breakage), 50 mg of nanofibers were shaken for 5 min with 5 mL of 70% ethanol. After complete fiber breakdown, visually confirmed by the absence of solid residues, 5 mL of hexane was added for complete homogenization, and the mixture was centrifuged (Eppendorf 5430 R Centrifuge, Germany) at 3226 × g for 5 min. The supernatant was collected and analyzed by GC-MS. The quantification of EOB compounds was expressed relative to the internal standard 1-nonanol (Sigma Aldrich) (0.2 mg/mL). The CC and EE of the electrospun HPMC nanofibers were calculated using Equations 3 and 4, respectively. The 14 quantified compounds, used to calculate loading capacity and encapsulation efficiency, are presented in Table 3.

Eq. 3

$$\mathrm{LC}\ (\%) = \frac{\mathrm{W_2}}{\mathrm{M}} \times 100\%$$

where W_2 is the total content of EO compounds (internal and external – due to nanofiber rupture), and M is the total content of EO compounds estimated in the nanofibers.

Eq. 4

$$\mathrm{EE}\ \ (\%) = \frac{\mathrm{W_2\text{-}W_1}}{\mathrm{W_2}} \times 100\%$$

where W_1 is the content of EO compounds in the solution (external washing of the nanofibers, without rupture), W_2 is the total content of EO compounds (internal and external – due to nanofiber rupture), and M is the total content of EO compounds estimated in the nanofibers.

2.13 Differential Scanning Calorimetry (DSC) of HPMC-EOB nanofibers

The thermal properties of nanofibers incorporating different concentrations (0, 5, 10, 15, and 20%) of EOB were evaluated using a DSC instrument (Q20, T.A. Instruments, USA). DSC was employed to provide information on the thermal behavior of the nanofibers. For this purpose, approximately 2.5 mg of each material was placed in hermetically sealed aluminum capsules (Shimadzu, code: 201-53090). The samples were heated at 10°C/min over the temperature range of 30°C to 300°C under a nitrogen flow of 50 mL/min.

2.14 Determination of antioxidant activity using the DPPH and ABTS assays for HPMC-EOB nanofibers

Analyses of antioxidant activity were performed using the DPPH (2,2-diphenyl-1-picrylhydrazyl) radical according to the methodology of Brand-Williams et al. (1995) and ABTS (2,2’-azino-bis(3-ethylbenzothiazoline-6-sulfonic acid)) according to Rufino et al. (2007), both with minor adaptations; for both methods, 30 mg of

sample was used per 2 mL of solvent (methanol and ethanol), respectively. The nanofibers were weighed in triplicate; solvents were added, followed by vortexing until the samples were completely homogenized; the solutions were then centrifuged at 4000 rpm for 20 minutes at 0°C to 4°C; finally, the supernatant was collected and the analysis performed. The results were expressed in µg of Trolox/g of sample, using Trolox as the standard. The samples were quantified using a spectrophotometer (SpectraMax 190, Molecular Devices, USA) at 515 nm and 734 nm for DPPH and ABTS, respectively.

2.15 *In vitro* antimicrobial activity of HPMC-EOB nanofibers

Nanofibers containing different concentrations (0, 5, 10, 15, and 20%) of EOB were used for antimicrobial analysis against bacterial strains, with results obtained from agar diffusion disc tests, MIC, and MBC conducted with free OEs. Thus, antimicrobial testing of the nanofibers was performed using the microatmosphere test with *Escherichia coli* (ATCC 25922 and INQS 00182) and *Staphylococcus aureus* (ATCC 10832), following the methodology proposed by Ghabraie et al. (2016) and Lemos et al. (2025), with adaptations. The inoculum was prepared as previously reported (Section 2.2.1). For the microatmosphere analysis, the nanofibers fixed on aluminum foil containing different concentrations (0, 5, 10, 15, and 20%) of EOB were cut (90 mm diameter) and evaluated for the action of the volatiles. The nanofibers were fixed to the top of the plates. Plates containing only bacterial growth were used as controls. The plates were sealed with parafilm and incubated upside down (lids facing down) at 37°C for 24 h. All treatments were performed in triplicate. After the incubation period, the colony-forming units (CFU) were counted. The results were expressed as the percentage reduction in microbial growth and calculated using Eq. 5.

Eq. 5

$$\text{Inhibition } (\%) = \frac{C\,c - C\,t}{C\,c} \times 100\%$$

where Cc is the growth of the control (without essential oil blend), and Ct is the growth of the treatment with essential oil blend.

2.16 *In vitro* antifungal activity of HPMC-EOB nanofibers

Nanofibers containing different concentrations (0, 5, 10, 15, and 20%) of EOB that showed positive results in the contact test conducted with free OEs were used for antifungal analysis in fungal cultures. The antifungal tests on the nanofibers were performed using the microatmosphere test with the fungi *Aspergillus flavus*, *Botrytis cinerea*, and *Penicillium crustosum*, following the methodology proposed by Ghabraie et al. (2016) and Lemos et al. (2025), with adaptations. After preparing the inoculum, the nanofibers fixed on aluminum foil containing different concentrations (0, 5, 10, 15, and 20%) of EOB were cut (90 mm in diameter) and evaluated for the effects of the volatiles on microatmosphere analysis. The nanofibers were fixed to the top of the plates. Plates containing only fungal growth were used as controls. The plates were sealed with parafilm and incubated upside down (lids facing down) at 25°C for 3 days. All treatments were performed in triplicate. After the incubation period, the colony-forming units (CFU) were counted. The results were expressed as a percentage reduction in microbial growth and calculated according to Eq. 5.

2.17 Statistical Analysis

The results were subjected to analysis of variance (ANOVA) and the Tukey test, and were reported as mean ± standard deviation, with a significance level of 5%. To evaluate the antifungal activity of the pure essential oils and the antimicrobial and antifungal activity of the nanofibers due to the action of volatile compounds, the data were subjected to analysis of variance (ANOVA), and the Kruskal-Wallis test was applied to compare means with a statistical significance level of $p \leq 0.05$, using the R Studio software (R version 4.4.2).

3 Results and Discussion

3.1 Agar diffusion disk test of essential oils (EOs)

The susceptibility of Gram-negative (*E. coli*) and Gram-positive (*S. aureus*) microorganisms was evaluated using the agar diffusion (AD) method, as well as minimum inhibitory concentration (MIC) and minimum bactericidal concentration (MBC) against lemongrass, clove, and thyme essential oils, as shown in Table 1. The EO from lemongrass and thyme exhibited the largest inhibition zones. Zones with diameters < 7 mm are considered to have low activity against bacteria, while those with diameters > 12 mm indicate a satisfactory inhibitory effect (Arora & Kaur, 1999; Souza et al., 2025).

The Gram-negative bacterium (*E. coli*) has a double-layered cell membrane (a cell envelope with an outer membrane rich in LPS, which reduces permeability to compounds) and is strongly hydrophobic, making it more resistant to antimicrobial agents compared to the single-layered membrane of the Gram-positive structure (*S. aureus*) (Smith-palmer et al., 1998). Thus, essential oils interact with cell envelopes of varying complexities, which impacts diffusion/penetration and the magnitude of the inhibitory effect. Other authors (Navikaite-Snipaitiene et al., 2025; Soltanzadeh et al., 2021) have also evaluated the antibacterial activity of lemongrass, clove, and thyme essential oils by measuring the minimum inhibitory concentration, the minimum bactericidal concentration, and inhibition zones via the agar diffusion assay, and found that these essential oils are particularly effective against *E. coli* and *S. aureus*, as in the present study. The agar diffusion method is a qualitative test for the initial evaluation of a substance's antimicrobial activity against a specific strain, requiring subsequent quantitative analysis using the MIC and MBC methods (Oliveira et al., 2021).

In the MIC and MBC tests, lemongrass essential oil showed values of 220 µl/mL for both *E. coli* and *S. aureus*, respectively (Table 1). Perdana et al. (2021) evaluated the antimicrobial effect of different essential oils, lemongrass, kaffir lime, finger-of-the-woman, and guava, all cultivated in Thailand. For lemongrass essential oil, the authors reported MIC values of 1.56 µl/mL for *E. coli* and 0.39 µl/mL for *S. aureus*, and for MBC, the reported data indicated values of 2.08 µl/mL against *E. coli* and 1.56 µl/mL against *S. aureus*. According to the authors, lemongrass essential oil exhibited the most effective MIC and MBC values among the essential oils tested, and the authors attributed this result to the active compound citral, which demonstrated inhibitory activity against foodborne pathogens, with a minimum inhibitory concentration (MIC) of 25–100 µg/mL.

Clove essential oil exhibited lower MIC/MBC values for *E. coli* (0.0080 µl/mL) than for *S. aureus* (0.07 µl/mL and 0.22 µl/mL, respectively), when compared to the effect of clove essential oil against *E. coli*, since the lower the value required to eliminate the microorganism, the more efficient the substance is. In the study by Pilong et al. (2023), the MIC of clove essential oil was tested against *E. coli*, *P. aeruginosa*, and *S. aureus*, and the results showed antimicrobial activity against all three bacteria. The authors reported that this may be due

to the action of the hydroxyl group of eugenol and other phenolic compounds present in clove essential oil (Ulanowska & Olas, 2021).

Thyme essential oil also exhibited a lower MIC for *E. coli* (0.02 µL/mL) than for *S. aureus* (0.06 µL/mL), and the MBC was lower for *S. aureus* (0.06 µL/mL) than for *E. coli* (0.67 µL/mL). As also reported by Al-Asmari et al. (2023), who tested the efficacy of thyme essential oil in inhibiting the growth of *S. aureus*, *E. coli*, and *S. cerevisiae* using MIC and MBC via the disk diffusion assay, the results were highly effective against the tested bacteria.

In comparison, clove and thyme essential oils exhibited a more pronounced inhibitory effect against *E. coli* and *S. aureus* than lemongrass essential oil. However, this study demonstrated antimicrobial activity against both tested bacteria, which may be due to the presence of phenolic and terpenoid compounds (eugenol in clove; thymol/carvacrol in thyme; citral/neral in lemongrass). The potent activity of bioactive compounds present in these essential oils likely plays a role in permeating bacterial defense mechanisms, leading to bactericidal effects (Schweitzer et al., 2022).

Table 1
Diffusion inhibition halos on agar (DA) and MIC and MBC against *E. coli* and *S. aureus* bacteria for lemongrass, clove and thyme essential oils.

Samples	**Inhibition halo (mm)**		**MIC***		**MBC***	
	E. coli	***S. aureus***	***E. coli***	***S. aureus***	***E. coli***	***S. aureus***
Lemongrass	27.00	60.00	220.00	220.00	220.00	220.00
Clove	19.33	48.67	0.0080	0.07	0.0080	0.22
Thyme	30.33	55.00	0.02	0.06	0.67	0.06

*MIC = Minimum Inhibitory Concentration, in µl/mL; MBC = Minimum Bactericidal Concentration, in µl/mL

3.3 Antifungal activity of essential oils (EOs) via contact action

The inhibitory effects of the three different EOs on the mycelial growth of the fungi *Aspergillus flavus*, *Botrytis cinerea*, and *Penicillium crustosum* via direct contact are presented in Table 2. Using direct contact as the mechanism of action, no significant difference ($p \geq 0.05$) was observed among the EO sources (lemongrass, clove, and thyme) at the different concentrations tested (1 and 0.6 µL/mL) against the fungus *Aspergillus flavus*. When comparing the essential oils at the same concentration, differences in fungal inhibition capacity were observed ($p \leq 0.05$). At concentrations of 1 and 0.6 µL/mL, lemongrass essential oil inhibited fungal growth by 100.0% at these concentrations, followed by thyme (93.7% and 86.4%) and clove (68.2% and 65.1%).

In the evaluation of essential oils against the fungus *Botrytis cinerea* at concentrations of 1 and 0.6 µL/mL, no significant difference ($p \geq 0.05$) was observed among the same sources of essential oils, with a 100.0% reduction for lemongrass and a 63.2% reduction for thyme in mycelial growth inhibition. Only in clove essential

oil was a significant difference ($p \leq 0.05$) observed among the different concentrations, with reductions of 100.0% and 92.1%, respectively. In the study by de Albuquerque Sousa et al. (2024) using clove essential oil, 100.0% fungal inhibition was also demonstrated at a concentration of 1.27 mg/L, highlighting its significant effect in combating *B. cinerea*. When comparing the essential oils at the same concentration, a significant difference was observed ($p \leq 0.05$). However, lemongrass EO did not differ statistically from clove EO at a concentration of 1 µL/mL.

For the essential oils against the fungus *Penicillium crustosum*, at concentrations of 1 and 0.6 µL/mL, no significant difference was observed ($p \geq 0.05$) among the same sources of essential oils, showing a reduction of 100.0% and 91.3% for lemongrass, 87.4%, and 76.3% for clove, and 89.5% and 83.2% for thyme, respectively, in terms of mycelial growth inhibition. When comparing the essential oils with each other at the same concentration, the lemongrass essential oil at concentrations of 1 and 0.6 µL/mL showed no significant difference ($p \geq 0.05$) from the clove and thyme essential oils. However, lemongrass EO at a concentration of 1 µL/mL showed a significant difference ($p \leq 0.05$) compared to clove and thyme EO. de Souza et al. (2024) tested the inhibitory effects of nine different essential oils against the mycelial growth of the fungus *Penicillium digitatum* after 72 h of incubation by direct contact, including clove and white thyme. Clove essential oil exhibited 100.0% inhibition of mycelial growth of *Penicillium digitatum* at a concentration of 1 µL mL^{-1}. In contrast, white thyme essential oil required a concentration higher than those used in this study (2 µL mL^{-1}) to inhibit fungal growth.

However, differences observed between the essential oils of the two tested fungi demonstrated that lemongrass essential oil exhibited a more pronounced inhibitory effect than clove and white thyme essential oils. da Cruz et al. (2023) identified the main compounds in lemongrass essential oil as α-citral (34.5%) and neral (25.3%), all of which belong to the monoterpene class and were described as the primary compounds of this essential oil with high antifungal activity, which corroborates the main compounds identified in the present study as shown in Table 3.

Table 2
Antifungal activity of lemongrass, clove and thyme essential oils against different fungi (*Aspergillus flavus*, *Botrytis cinerea* and *Penicillium crustosum*) and at different concentrations (1 and 0.6 µL/mL).

Sample	**Concentration (µL/mL)**	**Inhibition of mycelial growth (%)**		
		Aspergillus flavus	**Botrytis cinerea**	**Penicillium crustosum**
Lemongrass	1	100.00 ± 0.00^{a}	$100.00 \pm 0,00^{a}$	100.00 ± 0.00^{a}
Lemongrass	0.6	100.00 ± 0.00^{a}	100.00 ± 0.00^{a}	91.27 ± 16.02^{ab}
Clove	1	68.24 ± 3.07^{c}	100.00 ± 0.00^{a}	87.43 ± 3.18^{ab}
Clove	0.6	65.10 ± 5.84^{c}	92.15 ± 1.39^{b}	76.27 ± 1.68^{b}
Thyme	1	93.72 ± 2.62^{b}	63.18 ± 21.49^{c}	89.53 ± 4.80^{ab}
Thyme	0.6	86.39 ± 5.16^{b}	63.18 ± 11.49^{c}	83.25 ± 14.66^{b}

Averages followed by different letters in the same column indicate a significant difference in the concentrations and sources of essential oils by the Tukey test ($p \leq 0.05$).

3.4 Profile of volatile compounds in the blend of lemongrass, clove, and thyme essential oils (EOs)

Upon analyzing the chemical composition of the EOs (Table 3), 14 compounds were identified based on mass spectra and retention indices, accounting for 99.6% of the total. The bioactive compounds present in the highest percentages were α-citral (26.2%), eugenol (23.8%), neral (19.7%), and thymol (7.7%). In lemongrass essential oil, the main compounds reported in the literature are α-citral (34.5%) and neral (25.3%) (da Cruz et al., 2023), which are responsible for the characteristic citrus aroma (Guarda et al., 2011). These compounds are also related to the oil's biological properties, especially its antifungal activity (da Cruz et al., 2023).

For clove essential oil, eugenol is described as the major compound (55.3%), followed by (E)-β-caryophyllene (21.0%) and α-humulene (7.1%) (Liñán-Atero et al., 2024). The predominance of eugenol is often associated with the antioxidant properties, antimicrobial activity, and potential anti-inflammatory effects of this oil (Liñán-Atero et al., 2024).

Thyme essential oil, in turn, can contain up to 30 monoterpenes, resulting in a complex chemical composition that varies depending on the region of cultivation. Among the predominant compounds already reported are the chemotypes geraniol, alpha-terpineol, tuyanol-4, linalool, carvacrol, and thymol (Sakkas & Papadopoulou, 2017).

In general, it is observed that the blend preparation process preserved the main characteristic compounds of each essential oil used. Thus, the predominant bioactive compounds in the blend—α-citral and neral, derived from lemongrass, and eugenol, characteristic of clove oil—were preserved. Furthermore, the presence of thymol confirms the contribution of thyme essential oil to the final composition.

Table 3
Chemical composition of the essential oil blend (lemongrass, clove and thyme).

Nº	Fatty Acid	Formula	Similarity	Retention Time	Reference Ions	peak area (%)
1	Camphene	C10H16	96	3.22	93.10 (100%); 121.10 (74.11%); 79.05 (34.76%); 67.05 (29.65%); 107.10 (28.82 5)	0.65
2	5-Hepten-2-one, 6-methyl	C8H14O	97	3.57	43.00 9100%); 41.05 (53.92%); 108.10 (53.03%); 55.05 (38.58%); 69.05 (38.21%); 126.15^{+} (8.23%)	0.56
3	ρ-Cymene	C10H14	97	4.38	119.10 (100%); 134.15^{+} (32.98%); 91.05 (21.52%); 117.10 (12.71%); 120.10 (9.69%)	3.96
4	D-Limonene	C10H16	96		68.05 (100%); 67.05 (70.01%); 93.10 (67.24%)94.10 (31.91%); 79.05 (28.27%)	1.34
5	Linalool	C10H18O	98	5.95	71.05 (100%); 93.10 (81.24%); 41.00 (59.92%); 55.05 (59.76%); 43.00 (56.75%)	1.80
6	Neral	C10H16O	97	9.11	41.00 (100%); 69.05 (86.76%); 94.10 (30.37%); 84.05 (24.52%); 109.10 (22.19%)	19.75
7	Geraniol	C10H18O	97	9.72	69.05 (100%); 41.00 (69.42%); 68.05 (19.90%); 93.05 (14.56%); 67.05 (13.18%)	4.34
8	α-Citral	C10H16O	97	9.87	69.05 (100%); 41.05 (85.31%); 84.05 (27.77%); 94.10 (17.15%); 83.05 (10.55%)	26.21
9	Thymol	C10H14O	97	10.64	135.15 (100%); 150.15 (30.71%); 91.05 (15.15%); 115.05 (13.34%)	7.69
10	Eugenol	C10H12O2	98	12.05	164.00 (100%); 149.00 (36.84%); 77.00 (26.13%); 103.00 (24.12%); 131.00 (23.62%)	23.85
11	Geranyl acetate	C12H20O2	98	13.04	69.05 (100%); 41.00 (52.05%); 43.00 (46.10%); 68.05 (41.37%); 93.10 (27.26%)	3.34

Nº	Fatty Acid	Formula	Similarity	Retention Time	Reference Ions	peak area (%)
12	Caryophyllene	C15H4	97	14.11	93.10 (100%); 133.15 (91.69%); 69.05 (85.95%); 41.00 (77.89%); 91.05 (75.40%)	4.97
13	α-Caryophyllene	C15H24	96	14.93	93.10 (100%); 80.05 (32.58%); 121.10 (26.09%); 147.50 (20.43%); 92.10 (18.37%)	0.84
14	γ-Cadinene	C15H24	94	16.39	161.15 (100%); 105.05 (46.94%); 119.10 (38.13%); 91.05 (32.17%); 93.10 (28.50)	0.32

3.5 Electrical Conductivity and Rheology of HPMC Polymer Solutions with Different Concentrations of Essential Oil Blend

Electrical conductivity measures the ability of charges to migrate to the solution's surface, generating the electrostatic repulsive forces essential for jet formation during electrospinning (Vega-Lugo & Lim, 2012). In this regard, the conductivity of the solutions is an extremely important parameter, since low values may not induce sufficient charge on the surface of the Taylor cone, hindering jet formation (Haider et al., 2018).

Electrical conductivity was not significantly influenced ($p \geq 0.05$) in the HPMC polymer solutions incorporating 0, 5, and 10% essential oil blend (EOB) (Table 4). However, a significant reduction in conductivity ($p \leq 0.05$) was observed for solutions containing 15% and 20% EOB, which did not differ statistically from one another. Similar behavior was reported by de Souza et al. (2024), who observed a decrease in conductivity with increasing essential oil concentration, attributed to the hydrophobic nature of these compounds, which reduces ion mobility in the solution. On the other hand, Aydogdu et al. (2019) reported an increase in the dielectric constant in systems containing HPMC and soy protein, associated with an increase in charge density, an effect attributed to the presence of proteins and pH changes. This behavior differs from that observed in the present study, indicating that the composition of the polymer matrix and the nature of the additives significantly influence the system's electrical properties.

Modeling the rheological data using the Power Law model (Table 4) was appropriate for HPMC solutions containing EOB at concentrations ranging from 0 to 20%, with R^2 values ranging from 0.36 to 0.99, PI values ranging from 0.36 to 0.99, and P values ranging from 3.08 to 18.18%. For formulations containing 0, 5, and 10% EOB, the R^2 values were 0.99, while P ranged from 3.08 to 4.61%, indicating an excellent fit of the model to the experimental data. For the 15% EOB solution, a slight reduction in fit was observed ($R^2 = 0.92$; P = 6.32%), whereas for 20% EOB the model performed poorly ($R^2 = 0.36$; P = 18.18%), highlighting its limitations at higher concentrations.

The consistency index (K) values showed an increasing trend between 0 and 15% EOB, ranging from 38.54 to 64.17 $Pa \cdot s^n$, indicating greater resistance to flow and greater polymer network structuring. This behavior may be associated with interactions between phenolic and terpenoid compounds in the essential oils and the

hydroxyl and methoxyl groups of HPMC, favoring intermolecular associations. However, for the formulation containing 20% EOB, a reduction in the K value (57.25 Pa·s^n) was observed, possibly related to the formation of oil domains and the onset of phase separation, which compromises the continuity of the polymer matrix.

Simultaneously, a marked reduction in the flow index (n) was observed, from 0.45 to 0.07, maintaining values below 1 in all formulations, characterizing pseudoplastic behavior. The decrease in n indicates greater dependence of viscosity on the shear rate, which favors the alignment of polymer chains under an electric field. From the perspective of electrospinning, the combination of high K values and low n values is favorable for the formation of continuous nanofibers, as it provides sufficient viscosity to stabilize the jet and pseudoplastic behavior that facilitates stretching under an electric field. However, the reduction in conductivity associated with increased EOB concentration may limit the charge density in the jet, leading to instabilities such as flattening or the formation of non-uniform structures, especially at higher concentrations (15–20%). Similar behavior was reported by Bahrami et al. (2023) in solutions containing hydrophobic compounds, corroborating the Power Law model's influence on the interpretation of the rheological behavior of electrospun systems.

Table 4
Evaluation of polymeric solutions and nanofibers containing blends of essential oils (BEOs) at different concentrations.

BEOs (%)	**Evaluation of polymeric solutions**					**Fiber assessment**				
Parameters	**κ (mS·cm^{-1})**	**Power Law Model**				**D_{avg} (nm)**	**LC (%)**	**EE**	**θ_W (°)**	**Yield (%)**
		Performance								
K (Pa.s^n)	**n**	**R^2**	**P (%)**							
0	42.33 ± 0.50 [a]	38.54	0.45	0.99	4.51	62.96 ± 22.05[c]	-	-	11.21° ± 3.67[c]	95.85 ± 0.00 [a]
5	41.23 ± 1.33 [a]	47.86	0.41	0.99	3.08	74.84 ± 15.49[c]	58.45 ± 3.99[a]	94.19 ± 0.25[a]	36.11° ± 2.91[b]	50.26 ± 8.73 [b]
10	40.80 ± 0.36 [a]	47.97	0.37	0.99	4.61	128.62 ± 36.46[b]	12.06 ± 1.09[b]	82.00 ± 0.38[b]	54.53° ± 1.70[a]	36.34 ± 4.76 [bc]
15	38.00 ± 0.26 [b]	64.17	0.18	0.92	6.32	150.38 ± 45.34[a]	9.11 ± 0.75[b]	76.65 ± 0.46[c]	58.96° ± 3.10[a]	28.81 ± 0.95 [c]
20	36.67 ± 0.32 [b]	57.25	0.07	0.36	18.18	160.35 ± 38.02[a]	9.10 ± 0.87[b]	73.47 ± 1.16[d]	36.52° ± 4.67[b]	43.22 ± 1.64 [bc]

The results were expressed as the mean (n = 3) ± standard deviation., κ – electrical conductivity; K – apparent viscosity; n – fluid flow index; R^2 – coefficient of determination; Davg – average diameter; LC – charging

efficiency; EE – encapsulation efficiency; θW – static contact angle with water. Letters in the same column indicate a significant difference between the samples, according to Tukey's test ($p > 0.05$).

3.6 Yield from nanofiber production

The encapsulation yield of electrospun nanofibers containing different EOB concentrations (0, 5, 10, 15, and 20%) is presented in Table 4. Nanofibers production yield ranged from 28.81 to 95.85%.

The control treatment (0% EOB) showed the highest yield and differed significantly ($p \leq 0.05$) from all EOB - containing formulations. Among the incorporated samples, the treatment containing 5% EOB also differed significantly from the 15% formulation, whereas the other concentrations did not differ statistically from each other. The reduction in yield observed after EOB incorporation may be related to changes in the physicochemical properties of the polymer solutions.

As EOB concentration increased, electrical conductivity decreased from 42.33 to 36.67 mS cm^{-1}, while the flow behavior index (*n*) decreased from 0.45 to 0.07, indicating greater pseudoplastic behavior. In addition, the performance index increased from 4.51 to 18.18, suggesting less favorable electrospinning conditions. These changes likely affected jet stability during electrospinning, reducing the efficiency of fiber deposition on the collector.

This interpretation is supported by the increase in average fiber diameter from 62.96 nm in the control to 160.35 nm at 20% EOB. Furthermore, preliminary observations showed that concentrations above 20% resulted in film formation and solution dripping rather than continuous nanofibers, reinforcing the idea that higher EOB contents negatively affected process stability and, consequently, nanofibers yield.

3.7 Morphology and Size Distribution of HPMC-EOB nanofibers

The morphologies and average size distributions of HPMC nanofibers incorporating 0, 5, 10, 15, and 20% EOB are shown in Fig. 1. The HPMC nanofibers with 0, 5, and 10% EOB (Fig. 1) exhibited a cylindrical, homogeneous morphology without granules. However, the HPMC nanofibers with 15 and 20% EOB (Fig. 1D, E) exhibited a fibrous and flattened morphology, with these characteristics possibly attributed to incomplete solvent evaporation, which likely occurred only after deposition. Some authors reported similar characteristics during a study of the morphology of electrospun nanofibers made from poly(ε-caprolactone) (Hsu & Shivkumar, 2004). According to the authors, fibrous and flattened structures are obtained from wet nanofibers, which may indicate that the solvent had not yet completely evaporated when the fiber reached the collector, and under these conditions, they may also undergo redissolution and coalescence due to low viscosity. However, they were also found to be free of beads.

The average diameters (Davg) of the nanofibers (Table 4) at different EOB concentrations were 62.96 ± 22.05, 74.84 ± 15.49, 128.62 ± 36.46, 150.38 ± 45.34, and 160.35 ± 38.02 nm for nanofibers encapsulated with 0, 5, 10, 15, and 20% EOB, respectively. It was observed that the nanofibers with 0% and 5% EOB did not show a significant difference between them ($p \geq 0.05$), and the same behavior was observed in the nanofibers with 15% and 20% EOB. However, there was a significant increase ($p \leq 0.05$) in the average diameter of both the nanofibers with 15% and those with 20% EOB. This behavior may be associated with the electrical conductivity

of the solution (Table 4), which decreased significantly with increasing EOB concentration, thereby increasing the nanofibers diameter (Fig. 1). According to Bhardwaj & Kundu (2010), lower electrical conductivity of the polymer solution results in nanofibers with a larger average diameter. In addition to solution parameters, other factors contribute to the average fiber diameter, such as electrospinning conditions and parameters, as well as environmental conditions (Fonseca et al., 2020). Similar behavior regarding the average fiber diameter was observed by da Silva et al. (2025) when encapsulating linseed oil using HPMC and zein via electrospinning, in which an increase in oil concentration corresponded to an increase in the average fiber diameter.

3.8 Contact Angle of HPMC-EOB nanofibers

HPMC nanofibers exhibited a low contact angle with water (Table 4) of θ = 11.21˚ ± 3.67, θ = 36.11˚ ± 2.91, θ = 54.53˚ ± 1.70, θ = 58.96˚ ± 3.10 and θ = 36.52˚ ± 4.67 for nanofibers incorporating 0, 5, 10, 15 and 20% EOB, respectively. An increase in contact angles was observed with increasing EOB concentrations, due to reduced hydrophilicity (Fig. 2). However, this behavior was not linear due to the decrease in the contact angle in the fiber with 20% EOB, which may have occurred due to changes in the surface tension of the membrane, which affects its hydrophilicity, such as roughness, porosity, surface heterogeneity, morphology and oil exudation (da Silva et al., 2025). This increase observed in contact angles after the addition of EOB was expected due to the constituents of the nanofibers, since EOs are more hydrophobic than the hydroxypropyl methylcellulose polymer.

Similar behavior was reported by da Silva et al. (2025) when linseed oil was encapsulated by electrospinning using different concentrations of HPMC-zein. The authors observed an increase in the contact angle with increasing linseed oil concentration from 5% to 20% (w/w). The authors attribute this increase to the presence of the chemical constituents of the oil, which is composed of fatty acids and triacylglycerol, which has hydrophobic characteristics. However, the contact angles of the nanofibers produced in this study were less than 90˚, which is characteristic of hydrophilic behavior (Pires et al., 2024). The polymer used as wall material for fiber production was hydroxypropyl methylcellulose, a hydrophilic polymer (Ding et al., 2015). This material has hydrophilic characteristics, but it does not disintegrate/solubilize instantly due to the structure and interactions of the polymer and the morphology of the fibrous mat; in addition, the solvent used in production influences porosity and wettability, making the contact angle of the nanofibers extremely important for determining the type of food for application, due to the interactions of the bioactive compounds encapsulated in the nanofibers and their bioactive effect with the food (Pires et al., 2024).

3.9 Fourier Transform Infrared (FT-IR) Spectra of HPMC-EOB nanofibers

The Fourier transform infrared spectroscopy (FTIR) technique is used to characterize the chemical structure of the components and the main functional groups (Soltanzadeh et al., 2021). These results provide useful information about the trapping of EOs in the nanofibers.

The FTIR spectrum of the control fiber exclusively demonstrated the characteristic bands of HPMC (Fig. 3). The broad band between 3399 and 3442 cm^{-1} corresponds to the stretching of the O-H hydroxyl group, typical of the polymer (Aswathy et al., 2024). The band at 2906 cm^{-1} may be related to C-H vibrations (Ding et al.,

2015) due to the CH3 groups formed by the substitution of hydroxyls by methoxyl and hydroxypropyl groups (Dag et al., 2023). Furthermore, characteristic bands of cellulose derivatives were observed: 1645 cm^{-1} (indicating the C-O single bond of the six-carbon cyclic pyranose of HPMC) (Klangmuang & Sothornvit, 2016), 1448 cm^{-1} (CH3 asymmetric bending vibration), and 1060 cm^{-1} (C-O stretching vibration), associated with HPMC (Ding et al., 2015). These bands confirm that only HPMC groups are present in the control fiber.

The EOB showed bands absent in the control fiber. The bands present from 2852 to 2966 cm^{-1} are attributed to the stretching of the C-H groups of the terpenes (Jang et al., 2017). In addition, the EOBs showed a band at 1998 cm^{-1}, exclusive to the OEs. The 1453 cm^{-1} band was also observed, attributed to the methyl groups of the terpene compounds (Soltanzadeh et al., 2021). These bands are associated with the terpenic and aromatic groups characteristic of lemongrass, clove, and thyme essential oils.

The broad absorption band of 3399–3442 cm^{-1} (O-H) is cited for both HMPC and EOB. However, in nanofibers containing EOB, some bands were maintained and reflect the HPMC structure. The nanofibers maintained the bands attributed to the polymer in the region of 1052–1058 cm^{-1} and the shoulder at 939–946 cm^{-1}, observed in all nanofibers (except EOB). The band observed between 1052–1058 cm^{-1} can be attributed to the stretching of the C–O–C glycosidic bonds, characteristic of the structure of cellulose-derived polysaccharides (Kačuráková et al., 2000; Kačuráková & Wilson, 2001). Furthermore, the shoulder observed between 939–946 cm^{-1} may be related to vibrations of the pyranose ring and the polysaccharide ring skeleton, frequently reported in the 1000 – 920 cm^{-1} region for cellulosic materials (Poletto et al., 2014).

The nanofibers containing EOB showed new bands absent in the control fiber, demonstrating effective incorporation of the EOB mixture, the main objective of the present study. The bands between 2852–2966 cm^{-1}, referring to the C-H stretching of terpenes, were recorded in the nanofibers with EOB (Jang et al., 2017). The band at 1668–1671 cm^{-1}, more intense in the nanofibers with 15% and 20% EOB, was attributed to conjugated C = O bonds typical of terpenoids and phenols (Aswathy et al., 2024). The 1510–1516 cm^{-1} band, related to aromatic C = C bonds, also appeared only in nanofibers with EOB and in pure EOB (Rodríguez et al., 2018). The 1453 cm^{-1} band corresponds to the methyl groups of the terpene (Soltanzadeh et al., 2021). The 849–852 cm^{-1} bands are attributed to the = CH vibration of double bonds (Rodríguez et al., 2018). The bands absent in HPMC but present in nanofibers and EOB confirm the incorporation of aromatic, terpenic, and phenolic compounds characteristic of the blend.

3.10 Load Capacity (LC) and Encapsulation Efficiency (EE) of HPMC-EOB nanofibers

The LC and EE results for the electrospun nanofibers are presented in Table 4. The highest LC value was obtained for the nanofibers with 5% EOB (58.4 ± 4.0%), accompanied by a high EE (94.2 ± 0.2%). However, increasing the concentration of EOB resulted in a sharp reduction in LC, with values of 12.1 ± 1.1%, 9.1 ± 0.7%, and 9.1 ± 0.9% for oil loads of 10%, 15%, and 20%, respectively. At the same time, EE showed a decreasing trend, falling from 82.0 ± 0.4% to 73.5 ± 1.2% as the concentration of EOB increased.

This behavior suggests that, at higher oil concentrations, the polymer matrix reached its maximum load capacity, leading to inefficient encapsulation due to reduced encapsulation efficiency, and possible oil loss

during processing due to the high volatility of the EOs, which corroborates the results found in the fiber morphology of this study (Fig. 1), mainly at the higher concentrations of EOs (15 and 20%) used. Similar trends were reported by Pires et al. (2024), who observed a reduction in load capacity as the EO content in the nanofibers increased, attributing this effect to saturation of the polymer network, with load capacity varying from 44 to 54%. In the present study, the sharp decline in fiber load capacity from 5% (w/w) to 10% indicates that a concentration limit was exceeded, impairing the uniform distribution of oil within the nanofibers, and that the HPMC polymer was insufficient to retain larger amounts of oil.

Comparable results were also reported by Aydogdu et al. (2019), who encapsulated gallic acid in hydroxypropyl methylcellulose (HPMC) nanofibers by electrospinning. The authors found that loading efficiency was strongly influenced by interactions between the polymer and the active compound, reaching 69% in nanofibers containing 10% gallic acid relative to the polymer mass. It is important to note that in the present study, the amount of oil was calculated based on the mass of the polymer solution, and not on the mass of the dry polymer.

3.11 Differential Scanning Calorimetry (DSC) of HPMC-EOB nanofibers

Thermal analysis by differential scanning calorimetry (DSC) of HPMC nanofibers containing different concentrations of lemongrass, clove, and thyme essential oil (EOB) mixtures revealed changes in the thermal behavior of the developed material. According to Sundar & Parikh (2023), DSC is an important tool to confirm the encapsulation of active agents, such as essential oils, in polymeric matrices, as changes in the thermal peaks of the core or matrix indicate interactions and thermal stability of the system.

Pure EOB exhibited two distinct endothermic events (with peak temperatures (T_p) at ~ 148°C and 239°C) (Fig. 4), mainly associated with volatilization/evaporation and thermal transitions of the main major constituents, such as α-citral and neral (lemongrass), eugenol (clove), and thymol (thyme). This behavior reflects the nature of EO mixtures, composed of multiple constituents with different volatilities and thermal transition ranges, which explains the presence of multiple events in the thermogram (Melchior et al., 2023).

For the control HMPC nanofibers (0% EOB), an endothermic event with T_p at ~ 108°C is observed, mainly associated with the release of adsorbed water bound to the polymer structure and with structural rearrangements of the polymer matrix (Shetty et al., 2015; da Silva et al., 2025). This event is typical of cellulose derivatives, as their hydroxyl groups favor water retention. In pure HMPC, this event occurred in a temperature range of approximately 77°C to 117.9°C. Other authors have also observed an endothermic event in pure HPMC in the temperature range close to that found in this study, between 80°C and 117.9°C (Shetty et al., 2015; da Silva et al., 2025). In general, HMPC nanofibers incorporating 5%, 10%, and 15% EOB initially exhibit a small, underdeveloped endothermic event at lower temperatures. This event is also related to the release of adsorbed water/moisture from the HMPC and the thermal reorganization of the polymer matrix (da Silva et al., 2025). In these same nanofibers, at higher temperatures, a gradual decline in the baseline is observed, starting around ~ 130°C, attributed to the melting and/or volatilization of the EO compounds encapsulated in the polymer matrix. Unlike pure EOB (where two thermal events are visually well defined), in nanofibers this process occurs continuously and progressively, without a well-defined endothermic peak. This

behavior indicates that EO volatilization occurs gradually over a temperature range rather than at a single point, highlighting the preservation imposed by the polymeric matrix.

This thermal behavior after the incorporation of EOB into nanofibers indicates that the EOs are preserved by the HMPC matrix, which limits their mobility and modifies their thermal behavior. Furthermore, the absence of well-defined thermal events in the EOs of these nanofibers may be due to amorphization of the polymeric matrix, resulting in a disorganized structure in which the EO compounds remain homogeneously distributed. Studies indicate that matrix amorphization during the formation of encapsulated systems can hinder the identification of phase transitions in thermal analyses such as DSC (da Silva et al., 2025; Lim et al., 2022).

For nanofibers containing 20% BEOs, a more evident thermal event is observed at higher temperatures (T_p ~ 251°C), which can be attributed to the greater amount of incorporated compounds. At higher concentrations, some of the EOs may be present in less restricted regions of the polymer matrix, making the thermal event associated with the melting and/or volatilization of the compounds more pronounced. Clearly, the EO compounds that showed evident melting and/or volatilization events at T_p ~148 and ~ 239°C in pure EOB now occur together in a single event at a higher temperature, around T_p ~251°C, indicating that in the polymer matrix, there was an increase in the melting and volatilization temperature of the volatiles.

In general, the DSC results demonstrate that the incorporation of EOB alters the thermal profile of HMPC nanofibers, highlighting interactions between the EOs and the polymer matrix. The greater definition of thermal events in samples with higher EOB content confirms the influence of the concentration of encapsulated compounds on the thermal behavior of the system.

3.12 Determination of antioxidant activity using DPPH and ABTS assays of HPMC-EOB nanofibers

Essential oils contain terpenoids and phenols with antioxidant potential, such as those of lemongrass, clove, and thyme, which are important for application in food industry ingredients because they aid in food preservation related to the oxidation process, neutralizing free radicals that can damage food. Hydroxypropyl methylcellulose (HPMC) is a semi-synthetic polymer chemically modified from cellulose (Karnwal et al., 2025). In the present study, the DPPH and ABTS methods were used to evaluate the antioxidant capacity of pure EOs and incorporated nanofibers of the EO blend. The results of the analyses are shown in Figs. 5a and 5b.

According to the data presented in Fig. 5a, pure EOB and fiber with 20% EOB showed averages of 198.76 ± 0.99 and 192.69 ± 0.48 µg of Trolox/g of sample by the DPPH method, respectively, indicating the highest antioxidant activity and being statistically similar to each other, but superior to the others. The fiber with 15% EOB showed 177.47 ± 1.95 µg of Trolox/g of sample, demonstrating lower antioxidant activity than the others but still significantly higher than the samples with lower EOB concentrations, which showed a low response in terms of antioxidant activity. The control fiber (0% EOB) showed the lowest antioxidant activity capacity. It was observed that antioxidant activity was higher in samples with pure EOB and in fiber with 20% EOB, and that this activity decreased as the oil percentage in the fiber decreased.

The graph presented in Fig. 5b shows that the sample with pure EOB, with an average of 15.11 ± 0.12 µg of Trolox/g of sample by the ABTS method, has the highest antioxidant activity capacity, followed by the nanofibers with 20% EOB at 7.9 ± 0.06 µg of Trolox/g of sample. The nanofibers with 15% and 10% EOB, with averages of 7.38 ± 0.14 and 7.24 ± 0.28 µg of Trolox/g of sample, respectively, showed similar antioxidant activity capacity. The fiber with 5% EOB demonstrates even less potential for this activity, with an average of 5.76 ± 0.12 µg of Trolox/g of sample, and the control fiber showed practically no response for the ABTS.

Considering the results of the antioxidant activity analyses, it is noteworthy that nanofibers incorporating different concentrations of EOB showed better inhibition of the DPPH radical. It is also possible to observe that, in both assays, the nanofibers demonstrated similar behavior: as the concentration of EOB increased, the responses were more satisfactory in terms of inhibition of both radicals.

3.13 *In vitro* antimicrobial activity of HPMC-EOBs nanofibers

The nanofibers at different concentrations of EOB (0, 5, 10, 15 and 20%) inhibited the bacterial growth of *S. aureus* by 17.2%, 92.6%, 98.4%, 95.1% and 96.3% and of *E. coli* by 0.0%, 40.7%, 28.6%, 73.8% and 24.8%, respectively, when evaluated by micro atmosphere. The effect of the nanofibers against *S. aureus* is shown in Fig. 6; the samples containing fibers with 10% EOB showed the greatest inhibitory effect, followed by the other concentrations (0, 5, 15 and 20%). The application of EOB at different concentrations inhibited the percentage of *S. aureus* inhibition by almost 100%, proving the inhibitory capacity of the volatile components. No studies were found with electrospun HPMC containing specifically the blend used in the present study (50:25:25; lemongrass:clove:thyme). A possible explanation for the mechanism of action of essential oils, such as lemongrass, clove, and thyme essential oils, lies in their lipophilic characteristics. Lipophilic components bind to the phospholipid bilayer of the cell membrane and increase permeability, causing damage to the cellular enzymatic system by the intracellular content due to alterations in the cytoplasmic structure, directly affecting metabolism through the volatile compounds present in the essential oils (Peixoto et al., 2023).

Regarding the effect of the nanofibers against *E. coli* (Fig. 6), a non-linear response was observed, which may indicate heterogeneity of release/volatilization, corroborating the results found in the morphology, load capacity, and encapsulation efficiency of the nanofibers, mainly at the higher concentrations of EOB (15 and 20%). Nanofibers containing 5 and 20% EOB did not differ significantly ($p \geq 0.05$) in the *in vitro* evaluation of antimicrobial activity. Nanofibers containing 15% EOB exhibited a greater inhibitory effect, with a significant difference ($p \leq 0.05$) compared to the other EOB concentrations (5, 10, and 20%). Even though the other HPMC-EOB nanofibers amples showed lower antimicrobial activity, these results may also be attributed to the gradual release of the encapsulated EOB, since encapsulation promotes the gradual release of the compounds (Peixoto et al., 2023). Comparing the antibacterial effect of the tested nanofibers against *S. aureus* and *E. coli*, all exhibited a greater inhibitory effect against *S. aureus*. Some authors have reported that the antibacterial activity of essential oils depends on the structure of the bacterial cell wall, and that Gram-positive bacteria are more susceptible to essential oils than Gram-negative bacteria (Beikzadeh et al., 2020).

3.14 *In vitro* antifungal activity of HPMC-EOB nanofibers

The antifungal activity of nanofibers incorporated with a blend of essential oils (lemongrass, clove, and thyme), due to the action of volatiles, is shown in Fig. 7. The antifungal activity due to the action of volatile compounds increased proportionally with the increase in EOB concentration, with values of 19.1%, 59.6%, 77.7%, 80.8%, and 83.0% inhibition of mycelial growth against the fungus *Aspergillus*, 0.0%, 99.8%, 99.9%, 100%, and 100% against the fungus *Botrytis*, and 36.0%, 64.9%, 93.9%, 96.5%, and 100% against the fungus *Penicillium* for nanofibers containing 0%, 5%, 10%, 15% and 20% of EOB, respectively. Similar behavior was observed by de Souza et al. (2024) when different concentrations of clove and white thyme essential oils were added to octenylsuccinic anhydride-modified starch capsules, with reductions of 30.8% (2% clove EO), 46.2% (3% clove EO), 57.7% (4% clove EO), 31.7% (2% thyme EO), 38.5% (3% thyme EO), 51.0% (4% thyme EO).

Although all formulations showed antifungal properties against both fungi tested, the nanofibers containing 15% and 20% EOB exhibited the highest percentages of inhibition. For the fungus *Botrytis*, these nanofibers demonstrated greater inhibition of mycelial growth compared to *Aspergillus* and *Penicillium*, with 100% inhibition at the same concentrations of EOB used. The antifungal action of essential oils is related to their lipophilic characteristics, demonstrating that the effectiveness of essential oils in reducing fungal growth is related to their ability to penetrate the fungal cell wall (Chen et al., 2025). The results of this work confirm the antifungal activity of the EOB content incorporated into the nanofibers, making it promising for applications in the food sector as an additive or in food packaging.

4 Conclusions

The essential oils (EOs) of lemongrass, clove, and thyme in their free form exhibited antimicrobial activity against *E. coli* and *S. aureus* bacteria. Lemongrass and thyme EOs showed the largest inhibition halos. Regarding antifungal activity, lemongrass EO showed the greatest inhibitory effect against the mycelial growth of *Aspergillus flavus*, *Botrytis cinerea*, and *Penicillium crustosum* fungi by direct contact at the tested concentrations. The main volatile compounds identified in the blend of essential oils (EOB) were α-citral (26.21%), eugenol (23.85%), and neral (19.75%), respectively, maintaining the main compounds of each EO used in the blend.

The polymeric solutions exhibited pseudoplastic (non-Newtonian) behavior $n < 1$. The average diameter of the HPMC-based nanofibers, as a function of increasing EOB concentration, ranged from 62.96 to 160.35 nm under the adopted electrospinning conditions. The nanofibers exhibited a cylindrical, homogeneous morphology without beads, except at the highest concentrations (15–20%), where a tendency towards flattened fibers with hydrophilic behavior ($\theta < 90°$) was observed, as determined by water contact angle. The bands absent in HPMC, but present in the nanofibers and EOB, confirmed the incorporation of EOB into the HPMC nanofibers by the presence of bands associated with terpenic/phenolic constituents. The loading capacity of EOB in the 5% (w/w) nanofiber reached 58.4%, accompanied by high EE (94.2%). EOB demonstrated a thermal profile indicating greater retention of volatiles in the nanofibers than in the non-encapsulated form. Nanofibers with 20% EOB showed antioxidant activity (DPPH and ABTS) comparable to that of pure EOB under the assay conditions and in the adopted expression unit. Encapsulation of EOB conferred promising antimicrobial and antifungal activity to HPMC nanofibers through the action of the released volatile compounds, with concentrations of 10 and 15% EOB showing greater percentage reductions of *S. aureus* and *E. coli* in the microatmosphere assay. Specifically, HPMC nanofibers with 15 and 20% EOB

showed total inhibition against the *Botrytis* fungus under the tested conditions. Thus, HPMC nanofibers incorporated with EOB demonstrate potential for diverse applications in the food industry, such as active packaging components, volatile-emitting sachets/inserts, or polymeric matrices for controlled release, due to their functional properties and technological versatility. In situ studies in food matrices, release kinetics, storage stability, and sensory/toxicity/, and regulatory evaluations are necessary before industrial application.

Declarations

Conflict of Interest

We declare that there are no conflicts of interest.

Funding

This work was supported in part by the National Council for Scientific and Technological Development – Brazil (CNPq). This study was financed in part by the Coordenação de Aperfeiçoamento de Pessoal de Nível Superior – Brazil (CAPES) – Finance Code 001.

Author Contribution

L.P.V: Project administration, Conceptualization, Methodology, Data curation, Writing - original draft, Writing - review editing; K.G.S: Project administration, Conceptualization, Methodology, Data curation; C.J.A: Methodology, Writing – review & editing; E.P.C: Methodology, Writing – review & editing; T.J.S: Methodology, Writing – review & editing; G.C.P.G: Methodology, Writing – review & editing; T.S.S: Methodology, Writing – review & editing; L.V.C: Methodology, Writing – review & editing; F.T.S.S: Methodology, Writing – review & editing; G.N.R: Methodology, Writing – review & editing; E.R.Z: Resources, Methodology, Writing - review & editing, Supervision; D.M.O: Resources, Methodology, Writing - review & editing, Supervision; E.A.G: Resources, Methodology, Writing - review & editing, Supervision; L.N: Resources, Methodology, Writing - review & editing, Supervision; R.C.Z: Resources, Methodology, Writing - review & editing, Supervision.

Acknowledgement

This study was funded by the National Council for Scientific and Technological Development – CNPq and the Coordination for the Improvement of Higher Education Personnel – CAPES (code 001). We also thank the Southern Electron Microscopy Center (CEME-SUL) of FURG and the Laboratory of Innovation and Solutions in Chemistry, Research Group in Forensic Biosciences, of the Federal University of Pelotas for their availability to carry out the DSC analyses.

Data Availability

The datasets generated and analyzed during the current study are available from the corresponding author upon request. The data are not publicly available but can be provided to researchers for verification and further scientific use.

References

1. Al-Asmari, F., Koirala, P., Rathod, N. B., Alnemr, T. M., Asiri, S. A., Babeker, M. Y., Li, L., & Nirmal, N. P. (2023). Antimicrobial Activity of Formulated Origanum and Thyme Essential Oil Nanoemulsions - A Comparative Study. *Current Nutrition & Food Science*, *20*(6), 757–766. https://doi.org/10.2174/1573401319666230914140953
2. Al-Refaie, D., Mehyar, G. F., & Shahein, M. (2023). Functional Role of Essential Oils as Antimicrobial and Antioxidat Agents in Food Industry: A Review. *Jordan Journal of Agricultural Sciences*, *19*(1), 70–88. https://doi.org/10.35516/jjas.v19i1.1237
3. Arora, D. S., & Kaur, J. (1999). Antimicrobial activity of spices. *International Journal of Antimicrobial Agents*, *12*, 257–262. https://doi.org/10.1016/S0924-8579(99)00074-6
4. Aswathy, K. V., Beulah, K. C., Nalina, M., Sunil Ambedkar, D., Leela Sairam, A., Priyadarshini, P., Panneerselvam, A., & Rao, P. J. (2024). Hydroxypropyl methylcellulose stabilized clove oil nanoemulsified orodispersible films: Study of physicochemical properties, release profile, mucosal permeation, and anti-bacterial activity. *International Journal of Biological Macromolecules*, *283*. https://doi.org/10.1016/j.ijbiomac.2024.137577. Article e137577.
5. Aydogdu, A., Sumnu, G., & Sahin, S. (2019). Fabrication of gallic acid loaded Hydroxypropyl methylcellulose nanofibers by electrospinning technique as active packaging material. *Carbohydrate Polymers*, *208*, 241–250. https://doi.org/10.1016/j.carbpol.2018.12.065
6. Bahrami, Z., Pedram-Nia, A., Saeidi-Asl, M., Armin, M., & Heydari-Majd, M. (2023). Bioactive gliadin electrospinning loaded with *Zataria multiflora Boiss* essential oil: Improves antimicrobial activity and release modeling behavior. *Food Science & Nutrition*, *11*(1), 307–319. https://doi.org/10.1002/fsn3.3062
7. Beikzadeh, S., Akbarinejad, A., Swift, S., Perera, J., Kilmartin, P. A., & Travas-Sejdic, J. (2020). Cellulose acetate electrospun nanofibers encapsulating *Lemon Myrtle* essential oil as active agent with potent and sustainable antimicrobial activity. *Reactive and Functional Polymers*, *157*, Article e104769. https://doi.org/10.1016/j.reactfunctpolym.2020.104769
8. Bhardwaj, N., & Kundu, S. C. (2010). Electrospinning: A fascinating fiber fabrication technique. *Biotechnology Advances*, *28*, 325–347. https://doi.org/10.1016/j.biotechadv.2010.01.004
9. Bouqellah, N. A., Abdulmajeed, A. M., Alharbi, F. K. R., Mattar, E., Al-Sarraj, F., Abdulfattah, A. M., Hassan, M. M., Baazeem, A., Al-Harthi, H. F., Musa, A., Asseri, T. A. Y., & Soliman, M. H. (2025). Optimizing encapsulation of garlic and cinnamon essential oils in silver nanoparticles for enhanced antifungal activity against *Botrytis cinerea* pathogenic disease. *Physiological and Molecular Plant Pathology*, *136*. https://doi.org/10.1016/j.pmpp.2024.102522. Article e102522.
10. Brand-Williams, W., Cuvelier, M. E., & Berset, C. (1995). *Use of a Free Radical Method to Evaluate Antioxidant Activity*, *28*, 25–30. https://doi.org/10.1016/S0023-6438(95)80008-5
11. Chen, Y., Zhang, Y., Wang, L., Li, M., Wang, Y., Liang, J., Wang, D., Zhang, & Hai-wei. (2025).. Investigating the antifungal mechanism of *Artemisia argyi* essential oil against *Botrytis cinerea*, *Alternaria alternata*, and

Penicillium digitatum and its application in extending blueberry shelf life. *International Journal of Food Microbiology*, *439*, Article e111262. https://doi.org/10.1016/j.ijfoodmicro.2025.111262

12. CLSI. (2012). *Performance Standards for Antimicrobial Disk Susceptibility Tests; Approved Standard, Eleventh Edition. CLSI document M02-A11*. Clinical and Laboratory Standards Institute.
13. da Cruz, E. P., Pires, J. B., dos Santos, F. N., Fonseca, L. M., Radünz, M., Magro, D., Gandra, J., da Rosa Zavareze, E. A., E., & Dias, A. R. G. (2023). Encapsulation of lemongrass essential oil into cassava starch fibers for application as antifungal agents in bread. *Food Hydrocolloids*, *145*, Article e109105. https://doi.org/10.1016/j.foodhyd.2023.109105
14. da Silva, K. G., de Lima Costa, I. H., Alves, C. J., da Fonseca, B. A., da Cruz, E. P., Silva, F. T. S., dos Santos Teixeira, R., de Brito Leal, A., de Oliveira, G., Borges, C. D., da Rosa Zavareze, E., Nora, L., & Zambiazi, R. C. (2025). Encapsulation of linseed oil in ultrafine hypromellose-zein fibers by electrospinning: characterization and multivariate analysis. *International Journal of Biological Macromolecules*, *329*. https://doi.org/10.1016/j.ijbiomac.2025.147794. Article e147794.
15. da Silva Scudeler, C. G., de Lima Costa, T., Cortez-Vega, W. R., Prentice, C., & Fonseca, G. G. (2020). Development and characterization of Nile tilapia (*Oreochromis niloticus*) protein isolate-based biopolymer films incorporated with essential oils and nanoclay. *Food Packaging and Shelf Life*, *25*. https://doi.org/10.1016/j.fpsl.2020.100542. Article e100542.
16. Dag, D., Jung, J., & Zhao, Y. (2023). Development and characterization of cinnamon essential oil incorporated active, printable and heat sealable cellulose nanofiber reinforced hydroxypropyl methylcellulose films. *Food Packaging and Shelf Life*, *39*. https://doi.org/10.1016/j.fpsl.2023.101153. Article e101153.
17. de Albuquerque Sousa, T. C., da Cunha, W. M., Rosas, A. L. G., Oppelt, C. Q., Gandra, E. A., Rombaldi, C. V., & Meinhart, A. D. (2024). Essential oils as natural sources for the control of Botrytis cinerea: Chemical composition and antifungal effect. *Food Bioscience*, *62*. https://doi.org/10.1016/j.fbio.2024.105516. Article e105516.
18. de Oliveira Filho, J. G., Braga, A. R. C., de Oliveira, B. R., Gomes, F. P., Moreira, V. L., Pereira, V. A. C., & Egea, M. B. (2021). The potential of anthocyanins in smart, active, and bioactive eco-friendly polymer-based films: A review. *Food Research International*, *142*. https://doi.org/10.1016/j.foodres.2021.110202. Article e110202.
19. de Souza, E. J. D., Kringel, D. H., Siebeneichler, T. J., Rombaldi, C. V., Gandra, E. A., Dias, G., A. R., & da Zavareze, R., E (2024). Antifungal potential of clove and white thyme essential oils encapsulated in electrosprayed starch-OSA against *Penicillium digitatum*. *European Polymer Journal*, *215*. https://doi.org/10.1016/j.eurpolymj.2024.113192. Article e113192.
20. Ding, C., Zhang, M., & Li, G. (2015). Preparation and characterization of collagen/hydroxypropyl methylcellulose (HPMC) blend film. *Carbohydrate Polymers*, *119*, 194–201. https://doi.org/10.1016/j.carbpol.2014.11.057
21. do Moura, S., Rufino, M., Alves, R. E., de Brito, E. S., de Morais, S. M., de Goes Sampaio, C., Pérez-jiménez, J., & Saura-calixto, F. D. (2017). Metodologia científica: determinação da atividade antioxidante total em frutas pela captura do radical livre ABTSº+. Retrieved from

https://www.infoteca.cnptia.embrapa.br/bitstream/doc/426954/1/Cot128.*pdf*. Accessed January 6, 2026.

22. dos Santos, F. N., Fonseca, L. M., Alves, C. J., Crizel, R. L., Pires, J. B., Kroning, I. S., de Souza, J. F., Fajardo, A. R., Lopes, G. V., Dias, A. R. G., & da Zavareze, R., E (2024). Antimicrobial activity of geranium (*Pelargonium graveolens*) essential oil and its encapsulation in carioca bean starch ultrafine fibers by electrospinning. *International Journal of Biological Macromolecules*, *265*. https://doi.org/10.1016/j.ijbiomac.2024.130953. Article e130953.
23. Estevam, T. (2022). Avaliação do método de coacervação para produção de sistemas micro/nanoestruturados a base de derivados celulósicos. Retrieved from https://repositorio.ufu.br/handle/123456789/34267. Accessed January 6, 2026.
24. Fonseca, L. M., de Oliveira, J. P., Crizel, R. L., da Silva, F. T., da Rosa Zavareze, E., & Borges, C. D. (2020). Electrospun Starch Fibers Loaded with Pinhão (*Araucaria angustifolia*) Coat Extract Rich in Phenolic Compounds. *Food Biophysics*, *15*, 355–367. https://doi.org/10.1007/s11483-020-09629-9
25. Ghabraie, M., Vu, K. D., Tata, L., Salmieri, S., & Lacroix, M. (2016). Antimicrobial effect of essential oils in combinations against five bacteria and their effect on sensorial quality of ground meat. *LWT - Food Science and Technology*, *66*, 332–339. https://doi.org/10.1016/j.lwt.2015.10.055
26. Guarda, A., Rubilar, J. F., Miltz, J., & Galotto, M. J. (2011). The antimicrobial activity of microencapsulated thymol and carvacrol. *International Journal of Food Microbiology*, *146*(2), 144–150. https://doi.org/10.1016/j.ijfoodmicro.2011.02.011
27. Haider, A., Haider, S., & Kang, I. K. (2018). A comprehensive review summarizing the effect of electrospinning parameters and potential applications of nanofibers in biomedical and biotechnology. *Arabian Journal of Chemistry*, *11*(8), 1165–1188. https://doi.org/10.1016/j.arabjc.2015.11.015
28. Hsu, C. M., & Shivkumar, S. (2004). Nano-sized beads and porous fiber constructs of Poly(ε-caprolactone) produced by electrospinning. *Journal of Materials Science*, *39*(9), 3003–3013. https://doi.org/10.1023/B:JMSC.0000025826.36080.cf
29. Jafari, S., Sourki, A. H., & Pashangeh, S. (2025). Emulsion electrospinning of lemongrass essential Oil-Loaded *Ferula haussknechtii* gum/ Polyethylene oxide as bioactive coating. *Food Hydrocolloids for Health*, *7*. https://doi.org/10.1016/j.fhfh.2025.100195. Article e100195.
30. Jang, S., Jang, S., Lee, G., Ryu, J., Park, S., & Park, N. (2017). Halloysite Nanocapsules Containing Thyme Essential Oil: Preparation, Characterization, and Application in Packaging Materials. *Journal of Food Science*, *82*(9), 2113–2120. https://doi.org/10.1111/1750-3841.13835
31. Juliani, H. R., Simon, J. E., Quansah, C., Asare, E., Akromah, R., Acquaye, D., Asante-Dartey, J., Mensah, M. L. K., Fleischer, T. C., Dickson, R., Annan, K., & Mensah, A. Y. (2008). Chemical diversity of *lippia multiflora* essential oils from west africa. *Journal of Essential Oil Research*, *20*(1), 49–55. https://doi.org/10.1080/10412905.2008.9699420
32. Kačuráková, M., Capek, P., Sasinkova, V., Wellner, N., & Ebringerova, A. (2000). FT-IR study of plant cell wall model compounds: pectic polysaccharides and hemicelluloses. *Carbohydrate Polymers*, *43*, 195–203. https://doi.org/10.1016/S0144-8617(00)00151-X
33. Kačuráková, M., & Wilson, R. H. (2001). Developments in mid-infrared FT-IR spectroscopy of selected carbohydrates. *Carbohydrate Polymers*, *44*, 291–303. https://doi.org/10.1016/S0144-8617(00)00245-9

34. Karnwal, A., Kumar, G., Singh, R., Selvaraj, M., Malik, T.,al, & Tawaha, A. R. M. (2025). Natural biopolymers in edible coatings: Applications in food preservation. *Food Chemistry: X*, *25*. https://doi.org/10.1016/j.fochx.2025.102171. Article e102171.
35. Kieling, D. D., & Prudencio, S. H. (2019). Blends of lemongrass derivatives and lime for the preparation of mixed beverages: antioxidant, physicochemical, and sensory properties. *Journal of the Science of Food and Agriculture*, *99*(3), 1302–1310. https://doi.org/10.1002/jsfa.9305
36. Klangmuang, P., & Sothornvit, R. (2016). Barrier properties, mechanical properties and antimicrobial activity of hydroxypropyl methylcellulose-based nanocomposite films incorporated with Thai essential oils. *Food Hydrocolloids*, *61*, 609–616. https://doi.org/10.1016/j.foodhyd.2016.06.018
37. Laina, K. T., Drosou, C., & Krokida, M. (2024). Comparative assessment of encapsulated essential oils through the innovative electrohydrodynamic processing and the conventional spray drying, and freeze-drying techniques. *Innovative Food Science & Emerging Technologies*, *95*, Article e103720. https://doi.org/10.1016/j.ifset.2024.103720
38. Lemos, G. S., Vitoria, J. S., Fonseca, L. M., Pires, J. B., da Silva, F. T., Siebeneichler, T. J., de Oliveira Pacheco, C., Gandra, E. A., & da Rosa Zavareze, E. (2025). Active food packages for cake conservation: Antifungal potential of bean starch biodegradable films with orange peel essential oil. *International Journal of Biological Macromolecules*, *310*. https://doi.org/10.1016/j.ijbiomac.2025.143441. Article e143441.
39. Lim, L. M., Park, J. W., & Hadinoto, K. (2022). Benchmarking the Solubility Enhancement and Storage Stability of Amorphous Drug–Polyelectrolyte Nanoplex against Co-Amorphous Formulation of the Same Drug. *Pharmaceutics*, *14*(5). https://doi.org/10.3390/pharmaceutics14050979. Article e979.
40. Liñán-Atero, R., Aghababaei, F., García, S. R., Hasiri, Z., Ziogkas, D., Moreno, A., & Hadidi, M. (2024). Clove Essential Oil: Chemical Profile, Biological Activities, Encapsulation Strategies, and Food Applications. *Antioxidants*, *13*(4). https://doi.org/10.3390/antiox13040488. Article e488.
41. Magri, A., Ramos, M., Mellinas, C., Jiménez, A., & Garrigós, M. C. (2025). Encapsulation of lemongrass essential oil in cyclodextrins and maltodextrin: Antioxidant, antimicrobial and release studies. *Carbohydrate Polymer Technologies and Applications*, *10*. https://doi.org/10.1016/j.carpta.2025.100749. Article e100749.
42. Melchior, C., dos Santos Franciscato, L. M., Barbosa, V. A., da Silva, M. R., Bittencourt, P. R. S., Barros, B. C. B., Picolloto, A. M., & Moritz, C. M. F. (2023). Chemical composition and thermal properties of commercial essential oils and their antimicrobial and antioxidant activities. *Research Society and Development*, *12*(1), e39694. https://doi.org/10.33448/rsd-v12i1.39694
43. Navikaite-Snipaitiene, V., Rutkaite, R., Ivanauskas, L., Jakstas, V., Fieseler, L., Rüegg, N., & Yildirim, S. (2025). Development of thyme essential oil-based coatings and assessment of their antimicrobial activity. *Applied Food Research*, *5*(2). https://doi.org/10.1016/j.afres.2025.101367. Article e101367.
44. Peixoto, E. C., Fonseca, L. M., da Rosa Zavareze, E., & Gandra, E. A. (2023). Antimicrobial active packaging for meat using thyme essential oil (*Thymus vulgaris*) encapsulated on zein ultrafine fibers membranes. *Biocatalysis and Agricultural Biotechnology*, *51*, e102778. https://doi.org/10.1016/j.bcab.2023.102778
45. Perdana, M. I., Ruamcharoen, J., Panphon, S., & Leelakriangsak, M. (2021). Antimicrobial activity and physical properties of starch/chitosan film incorporated with lemongrass essential oil and its application.

LWT – Food Science and Technology, *141*, e110934. https://doi.org/10.1016/j.lwt.2021.110934

46. Pilong, P., Mishra, D. K., Ruengdech, A., & Siripatrawan, U. (2023). Foam-mat freeze-drying approach for preserving stability and antimicrobial activity of clove essential oil nanoemulsion. *Food Bioscience*, *52*. https://doi.org/10.1016/j.fbio.2023.102369. Article e102369.
47. Pires, J. B., dos Santos, F. N., da Cruz, E. P., Fonseca, L. M., Siebeneichler, T. J., Lemos, G. S., Gandra, E. A., da Rosa Zavareze, E., & Dias, A. R. G. (2024). Starch extraction from avocado by-product and its use for encapsulation of ginger essential oil by electrospinning. *International Journal of Biological Macromolecules*, *254*. https://doi.org/10.1016/j.ijbiomac.2023.127617. Article e127617.
48. Poletto, M., Ornaghi, H., & Zattera, A. J. (2014). Native cellulose: structure, characterization and thermal properties. *Materials*, *7*(9), 6105–6119. https://doi.org/10.3390/ma7096105
49. Rodríguez, J. D. W., Peyron, S., Rigou, P., & Chalier, P. (2018). Rapid quantification of clove (*Syzygium aromaticum*) and spearmint (*Mentha spicata*) essential oils encapsulated in a complex organic matrix using an ATR-FTIR spectroscopic method. *Plos One*, *13*(11). https://doi.org/10.1371/journal.pone.020740. Article e0207401.
50. Sakkas, H., & Papadopoulou, C. (2017). Antimicrobial activity of basil, oregano, and thyme essential oils. *Journal of Microbiology and Biotechnology*, *27*(3), 429–438. https://doi.org/10.4014/jmb.1608.08024
51. Schweitzer, B., Balázs, V. L., Molnár, S., Szögi-Tatár, B., Böszörményi, A., Palkovics, T., Horváth, G., & Schneider, G. (2022). Antibacterial Effect of Lemongrass (*Cymbopogon citratus*) against the Aetiological Agents of Pitted Keratolyis. *Molecules*, *27*(4), e1423. https://doi.org/10.3390/molecules27041423
52. Shamene, B., Tee, S. M., & Rosli, N. A. (2024). Strategic addition of rosemary essential oil in natural rubber-toughened poly (lactic acid)/cinnamon oil blends for antimicrobial packaging. *Future Foods*, *10*, Article e100506. https://doi.org/10.1016/j.fufo.2024.100506
53. Shetty, G. R., Rao, B. L., Asha, S., Wang, Y., & Sangappa, Y. (2015). Preparation and characterization of silk fibroin/hydroxypropyl methyl cellulose (HPMC) blend films. *Fibers and Polymers*, *16*, 1734–1741. https://doi.org/10.1007/s12221-015-5223-z
54. Smith-Palmer, A., Stewart, J., & Fyfe, L. (1998). Antimicrobial properties of plant essential oils and essences against five important food-borne pathogens. *Letters in Applied Microbiology*, *26*(2), 118–122. https://doi.org/10.1046/j.1472-765X.1998.00303.x
55. Soltanzadeh, M., Peighambardoust, S. H., Ghanbarzadeh, B., Mohammadi, M., & Lorenzo, J. M. (2021). Chitosan nanoparticles encapsulating lemongrass (*Cymbopogon commutatus*) essential oil: Physicochemical, structural, antimicrobial and in-vitro release properties. *International Journal of Biological Macromolecules*, *192*, 1084–1097. https://doi.org/10.1016/j.ijbiomac.2021.10.070
56. Souza, A. S., Borges, C. D., Radünz, M., Gandra, T. K. V., da Costa, D. A., Borba, C. S., Mendonça, C. R. B., & Gandra, E. A. (2025). Encapsulation of thyme essential oil (*Thymus vulgaris*) in chia mucilage (*Salvia hispanica* L.) and its application in fresh pork sausage. *International Journal of Biological Macromolecules*, *285*. https://doi.org/10.1016/j.ijbiomac.2024.138284. Article e138284.
57. Sundar, S. K., & Parikh, J. K. (2023). Advances and trends in encapsulation of essential oils. *International Journal of Pharmaceutics*, *635*. https://doi.org/10.1016/j.ijpharm.2023.122668. Article e122668.
58. Tao, N., Jia, L., & Zhou, H. (2014). Anti-fungal activity of Citrus reticulata Blanco essential oil against *Penicillium italicum* and *Penicillium digitatum*. *Food Chemistry*, *153*, 265–271.

https://doi.org/10.1016/j.foodchem.2013.12.070

59. Ulanowska, M., & Olas, B. (2021). Biological Properties and Prospects for the Application of Eugenol—A Review. *International Journal of Molecular Sciences*, *22*(7), e3671. https://doi.org/10.3390/ijms22073671
60. Vega-Lugo, A., & Lim, L. (2012). Effects of poly(ethylene oxide) and pH on the electrospinning of whey protein isolate. *Journal of Polymer Science Part B: Polymer Physics*, *50*(16), 1188–1197. https://doi.org/10.1002/polb.23106
61. Vitoria, J. S., Fonseca, L. M., Siebeneichler, T. J., Campos, D., Poças, F., Pintado, M. M. E., da Rosa Zavareze, E., & Gandra, E. A. (2025). Active Bilayer Material Formed by Starch Film and Thyme Essential Oil Encapsulated into Zein Electrospun Fibers. *Food and Bioprocess Technology*, *18*, 9438–9460. https://doi.org/10.1007/s11947-025-03959-7
62. Wen, P., Wen, Y., Zong, M. H., Linhardt, R. J., & Wu, H. (2017). Encapsulation of Bioactive Compound in Electrospun Fibers and Its Potential Application. *Journal of Agricultural and Food Chemistry*, *65*(42), 9161–9179. https://doi.org/10.1021/acs.jafc.7b02956

Figures

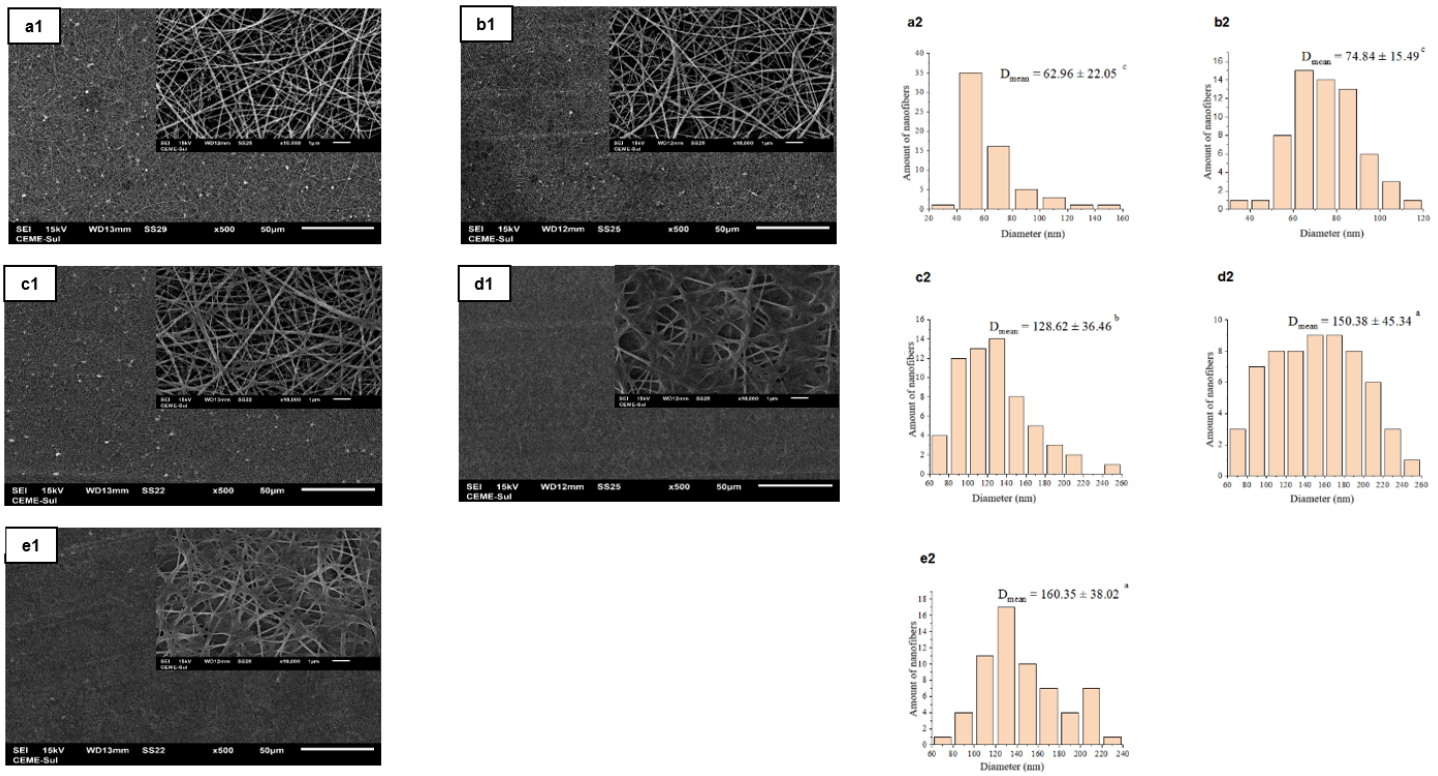


Figure 1

Scanning electron microscopy (SEM) of HPMC nanofibers incorporated with essential oil blend (lemongrass, cloves and thyme) a1 (0%), b1 (5%), c1 (10%), d1 (15%) and e1 (20%). Distribution of the average diameters (Dmed) of the nanofibers HPMC fibers incorporated with essential oil blend a2 (0%), b2 (5%), c2 (10%), d2 (15%) and e2 (20%).

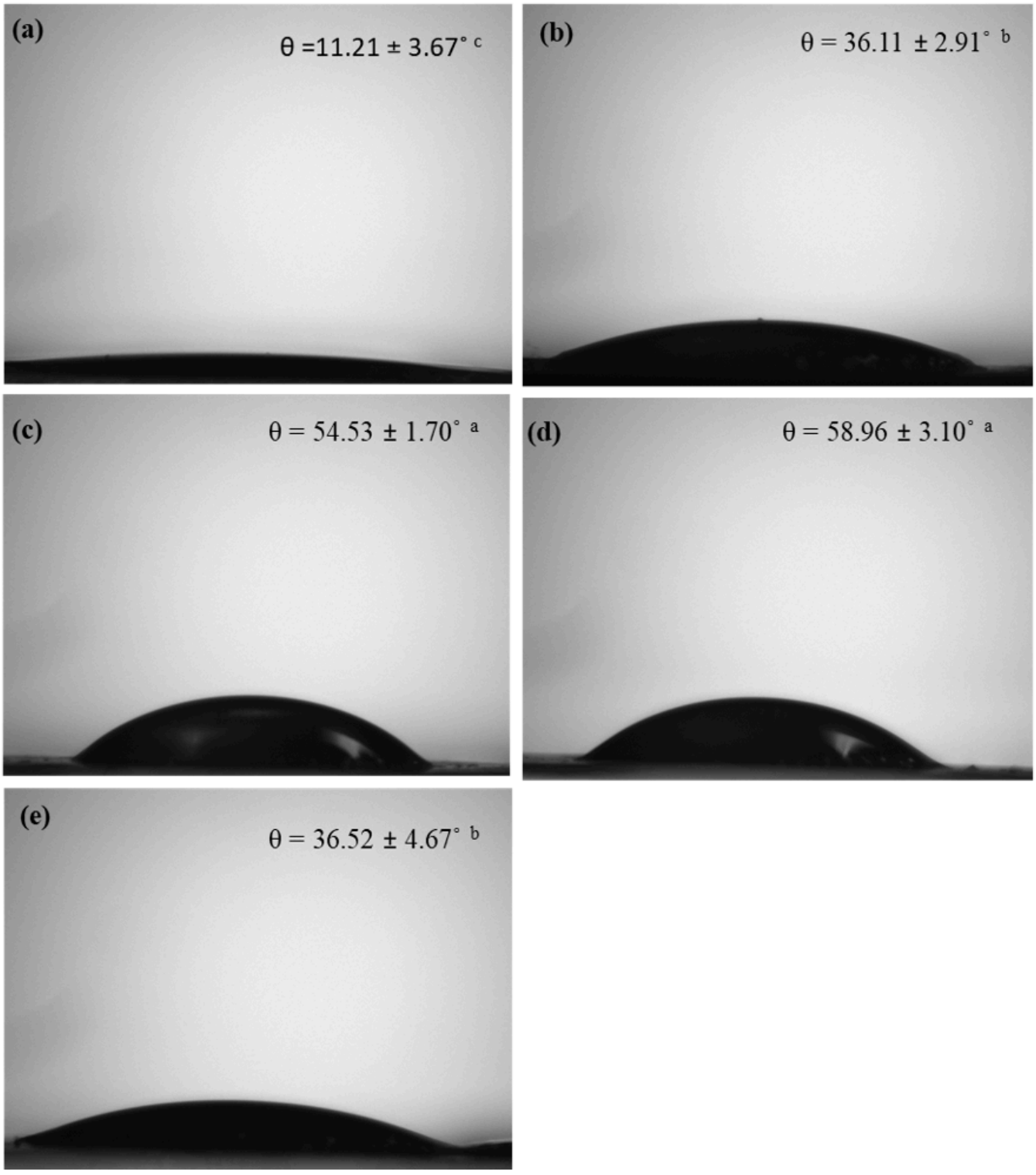


Figure 2

Static contact angle of the solid-liquid interface between the nanofibers membrane (0, 5, 10, 15 and 20%) and the model liquid, ultrapure water (θw).

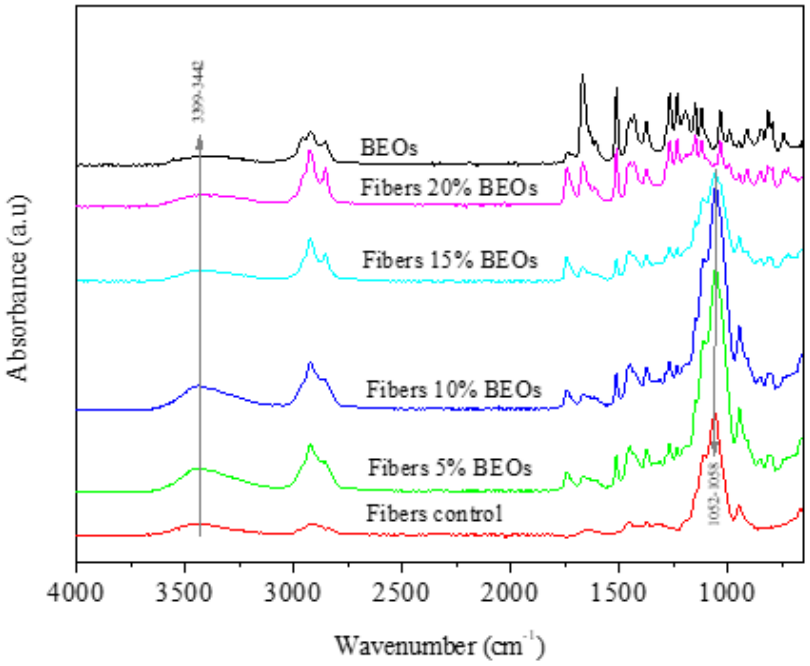


Figure 3

FTIR spectra of essential oil blend (lemongrass, cloves and thyme) of HPMC nanofibers incorporated with different concentrations of essential oil blend (lemongrass, cloves and thyme) 0, 5, 10, 15 and 20%.

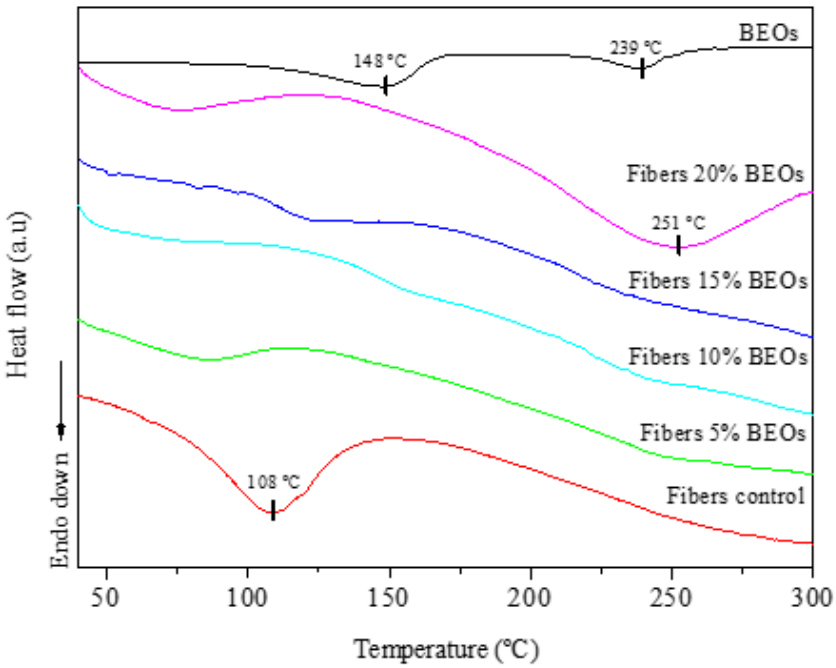


Figure 4

DSC thermograms of unencapsulated essential oil blend (lemongrass, cloves and thyme) encapsulated of essential oil blend, HPMC polymers and HPMC nanofibers incorporated with different concentrations of essential oil blend 0, 5, 10, 15 and 20%.

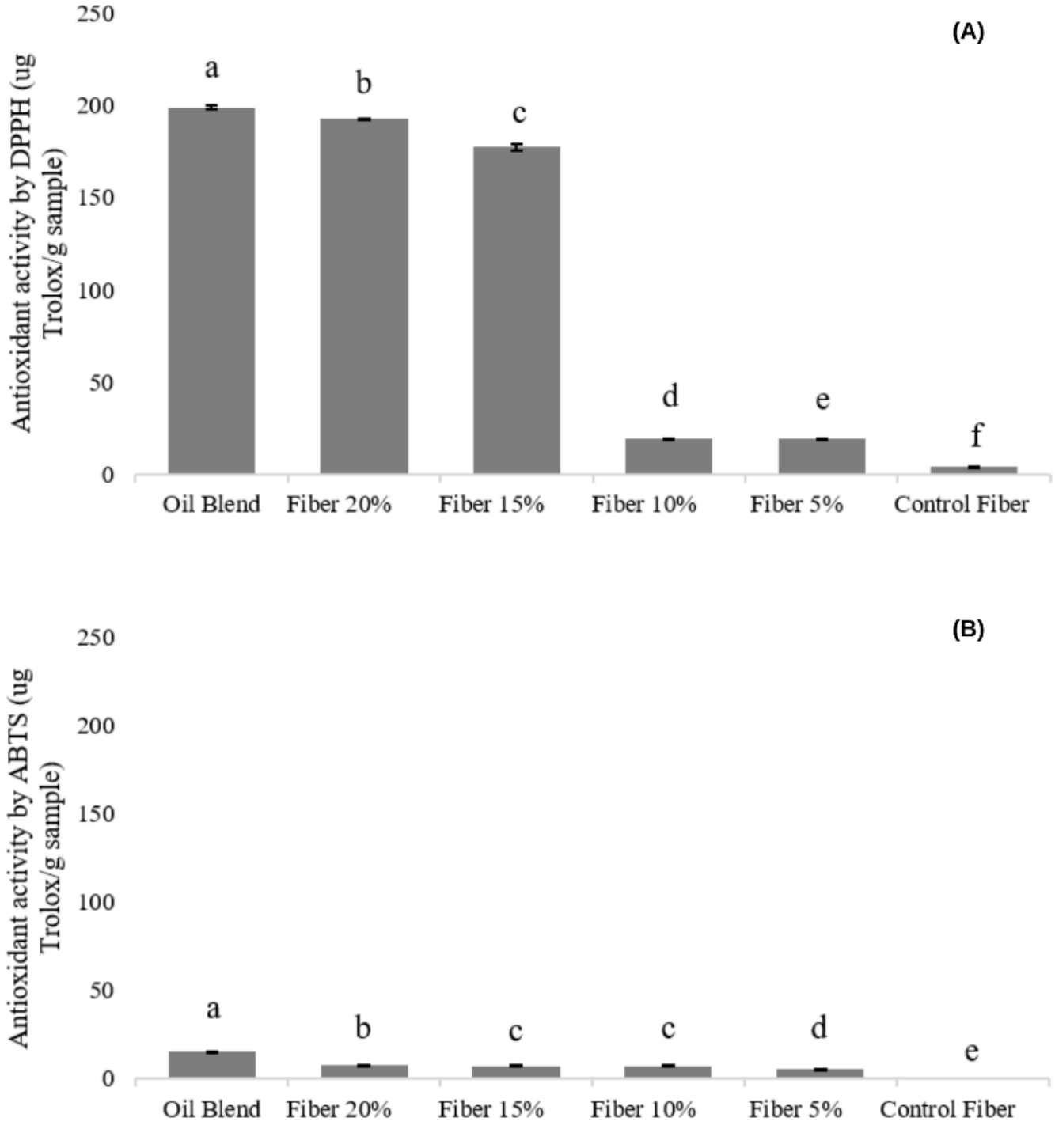


Figure 5

Graph of Antioxidant Activity Determination by (a) DPPH and (b) ABTS in essential oil blend (lemongrass, cloves and thyme) and nanofibers with different concentrations of essential oil blend 0, 5, 10, 15 and 20%.

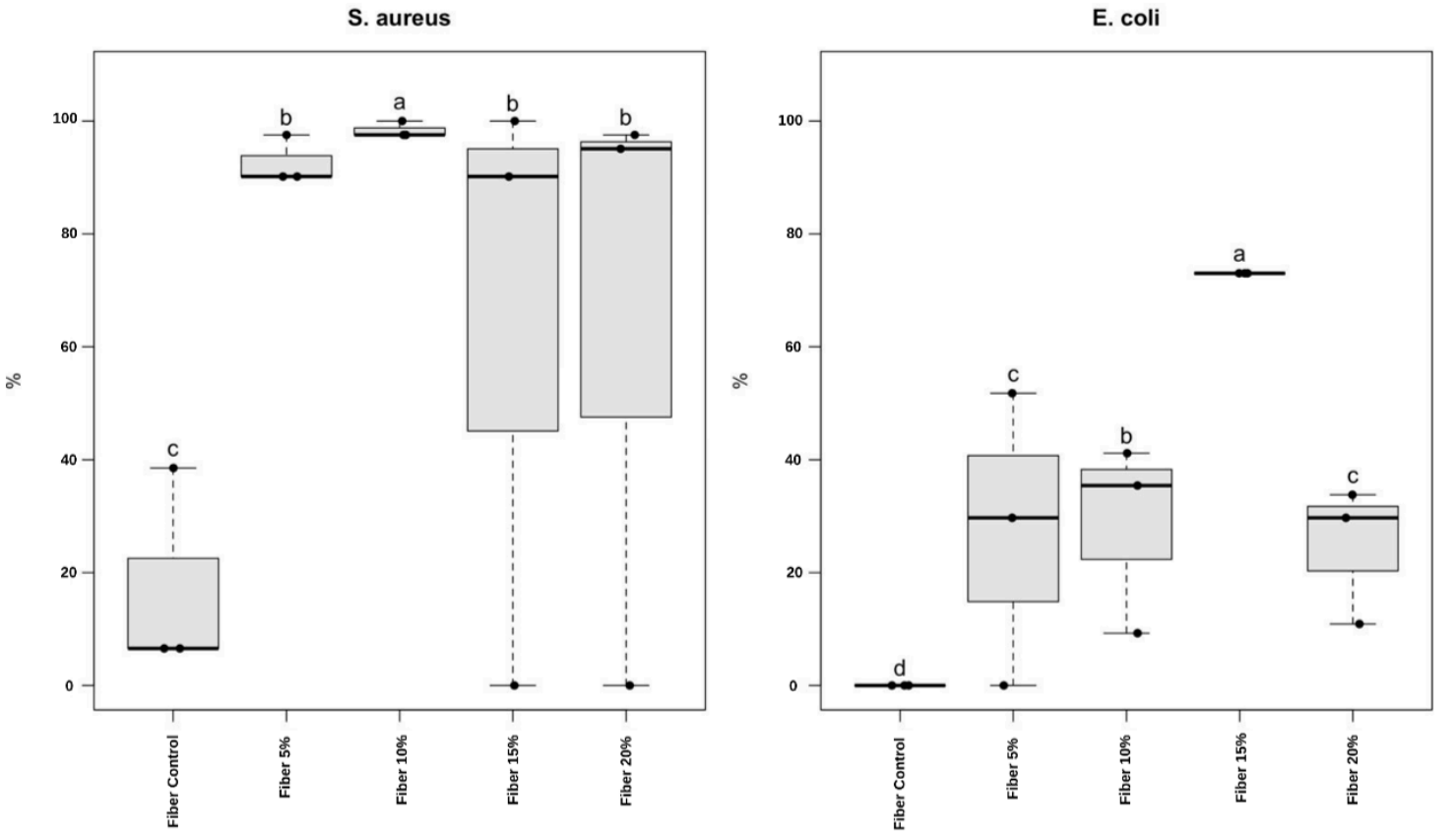


Figure 6

Inhibitory effect of nanofibers of HPMC incorporated with different concentrations of essential oil blend (lemongrass, cloves and thyme) 0, 5, 10, 15 and 20% on the growth of *Staphylococcus aureus* and *Escherichia coli*. Distinct letters indicate statistically different groups according to the Kruskal–Wallis test followed by Dunn's post-hoc test (Bonferroni-adjusted, $p < 0.05$).

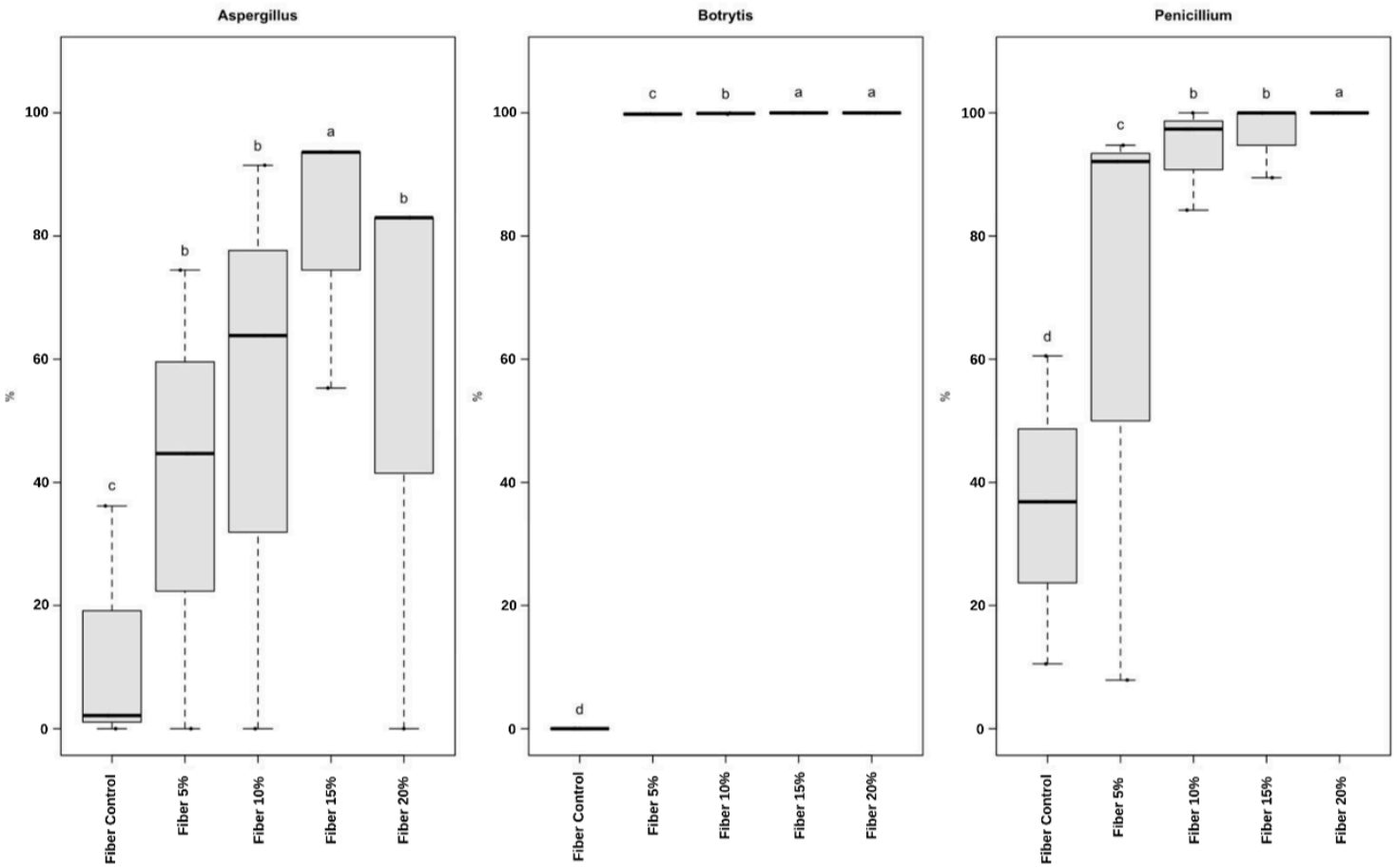


Figure 7

Inhibitory effect of nanofibers of HPMC incorporated with different concentrations of essential oil blend (lemongrass, cloves and thyme) 0, 5, 10, 15 and 20% on the growth of *Aspergillus*, *Botrytis*, and *Penicillium*. Distinct letters indicate statistically different groups according to the Kruskal–Wallis test followed by Dunn's post-hoc test (Bonferroni-adjusted, $p < 0.05$).